Activation of Atlantic cod (*Gadus morhua*) retinoid X receptors by organic tin compounds

Annichen Prebensen

Master of Science in Biology – Environmental toxicology

Department of Biological Sciences

University of Bergen

Spring 2023

Supervisors: Odd André Karlsen and Anders Goksøyr

Acknowledgements

This master thesis has been part of the iCod 2.0 project (project no. 244564) and dCod 1.0. project (project no. 248840) funded by the Research Council of Norway.

First and foremost, I would like to thank my supervisors Odd André Karlsen and Anders Goksøyr, for your help, support and enthusiasm in my work both in the laboratory and in the writing process. I would like to further extend my gratitude towards Odd André, for always taking the time to answer my questions and for the guidance and advice throughout this process. I would also like to thank the environmental toxicology group, for motivating and giving me feedback on my work. I also truly appreciate the opportunity for participating and presenting my work at the NSFT Winter meeting in Beitostølen January 2023.

I would also like to thank Rhîan Gaenor Jacobsen for teaching and helping me in the laboratory. I am truly grateful for your patience, encouragement and that you were always available to help when needed.

Lastly, I would like to thank my fellow students, friends and family for the immense support and motivation. I also want to give extra appreciation to Shaun for the support and encouragement throughout this year.

Bergen, 2023

Annichen Prebensen

Table of contents

Acknowledgements I
Table of contents II
Abbreviations V
Abstract VII
1. Introduction 1
1.1 Environmental pollutants 1
1.2 Organic tin compounds (OTCs) 2
1.2.1 Organotin toxicity 5
1.3 Nuclear receptors 6
1.4 Retinoid X receptor (RXR) 7
1.4.1 Subtypes and roles 7
1.4.2 RXR protein structure 9
1.4.3 RXR endogenous ligands 10
1.4.4 RXR exogenous ligands 10
1.5 Atlantic cod 11
1.5.1 Atlantic cod Rxr 12
1.6 Aim of the study 13
2. Materials 14
2.1 Reagents and chemicals 14
2.2 Plasmids 15
2.3 Enzymes 16
2.4 Primers 16
2.5 Cell lines 17
2.6 Growth medium 17
2.7 Buffers and solutions 18
2.7.1 Agarose gel 18
2.7.2 Luciferase gene reporter assay 18
2.7.3 Cell viability and cytotoxicity assay 19
2.7.4 Western blot assay 19
2.8 Kits 21
2.9 Instruments 22
2.10 Software 22
3. Methods 23
3.1 Experimental outline 23
3.2 RNA extraction 24
3.4 Complementary DNA (cDNA) synthesis 25
3.5 Polymerase chain reaction 26

3.6 Construction of pSC-B-gmRxr plasmid by blunt-end PCR cloning 26
3.6.1 Primers and PCR amplification of Rxr sequence from cDNA 26
3.7 Agarose gel electrophoresis 28
3.8 Gel extraction of DNA 28
3.9 Blunt PCR cloning 29
3.9.1 *Escherichia coli* transformation 29
3.9.2 Blue-white colony screening 30
3.9.3 Colony PCR 30
3.9.4 Plasmid purification 32
Construction of pCMX-GAL4-gmRxr 32
3.9.5 Restriction enzyme digestion 32
3.9.6 Ligation of gmRxr and pCMX-GAL4 33
3.9.7 Transformation of plasmid construct 34
3.9.8 Sanger sequencing 35
3.9.9 Plasmid purification - midiprep 36
3.10 Multiple sequence alignment 36
3.11 Western blot assay 36
3.11.1 Sodium-dodecyl-sulfate (SDS)-polyacrylamide gel electrophoresis (PAGE) 36
3.11.2 Preparation of cell lysates 37
3.11.3 Protein staining 37
3.11.4 Western blotting 37
3.12 Luciferase reporter gene assay 38
3.12.1 Cultivation of COS-7 cells 39
3.12.2 Seeding of COS-7 cells 40
3.12.3 Transfection of COS-7 cells 40
3.12.4 Ligand exposure of COS-7 cells 41
3.12.5 Reading – lysis and enzymatic measurements 42
3.13 Cell viability assay 43
4. Results 44
4.1 Cloning of gmrxra and gmrxrb2 and construction of eukaryotic expression plasmids 44
4.1.1 RNA extraction and cDNA synthesis 44
4.1.2 PCR amplification of gmRxra-hinge-LBD and gmRxrb2-hinge-LBD 45
4.1.3 Blunt-end PCR cloning and construction of pSC-B-gmRxra/b2-hinge-LBD plasmids 45
4.1.4 Sequencing pSC-B-Rxra/b2-hinge-LBD plasmids 46
4.1.5 Construction of the pCMX-GAL4-Rxra/b2/b2d-hinge LBD expression plasmids 46
4.2 Confirmation of GAL4-Rxra/b2-hinge-LBD fusion protein synthesis in transfected COS-7 cells 49
4.3 Luciferase reporter gene assay 50
4.3.1 Ligand activation of gmRxra/b1/b2/b2g/g-hinge-LBD 51
4.3.2 Differences in Rxr-LBD sequences between Atlantic cod and zebrafish 53

4.4 Cytotoxicity and cell viability 55
5. Discussion 57
5.1 Cloning of gmRxra and gmRxrb2, and identification of an Rxrb2 splice variant (gmRxrb2d) .. 57
5.2.1 Activation of gmRxra/b1/b2/b2d/g by 9-cis retinoic acid 58
5.2.2 Activation of gmRxra/b1/b2/b2d/g by organotins 59
5.2.3 Differences in amino acid sequences that affect ligand binding 61
5.3 Conclusion 62
5.4 Future perspectives 63
6. References 64
Appendix 71

Abbreviations

9-cis RA	9-cis retinoic acid
AF-1	Activation function 1
AF-2	Activation function 2
bp	Base pair
cDNA	Complementary deoxyribonucleic acid
CYP	Cytochrome P450
DBD	DNA-binding domain
DNA	Deoxyribonucleic acid
DDT	Dichlorodiphenyltrichloroethane
DHA	Docosahexaenoic acid
DMEM	Dulbecco's modified eagle medium
DMSO	Dimethyl sulfoxide
dNTP	Deoxynucleotides
EC_{50}	Half maximal effective concentration
E. coli	*Escherichia coli*
EDCs	Endocrine disruptive compounds
EDTA	Ethylenediaminetetraacetic acid disodium salt hydrate
EGTA	Ethylene glycol-bis(2-aminoethylether)-N,N,N',N'-tertacetic acid
E_{max}	Maximum efficacy
ER	Estrogen receptor
FBS	Fetal bovine serum
FC	Fentin chloride
FH	Fentin hydroxide
gmRxr	*Gadus morhua* Rxr
hRXR	*Homo sapiens* RXR
kDa	Kilo Daltons
LBD	Ligand binding domain
LBP	Ligand binding pocket
LOEC	Lowest observed effect concentration
MSA	Multiple sequence alignment
NR	Nuclear receptors
ODV	Optical density volume
ONPG	Ortho-2-nitrophenyl-B-D-galactopyranoside
OTC	Organotin
PA	Phytanic acid
PBS	Phosphate-buffered saline
PCB	Polychlorinated biphenyl
PCR	Polymerase chain reaction
PFAS	Per- and polyfluoroalkyl substances
PMSF	Phenylmethylsulfonyl fluoride
POPs	Persistant organic pollutants
PPAR	Peroxisome proliferator activated receptor
PR	Progesterone receptor
PVC	Polyvinyl chloride
PXR	Pregnane X receptor
qPCR	Quantitative polymerase chain reaction

RAR	Retinoic acid receptor
RNA	Ribonucleic acid
RPM	Revolutions per minute
RXR	Retinoid X receptor
SAP	Shrimp alkaline phosphatase
SDS	Sodium-dodecyl-sulfate
SDS-PAGE	Sodium-dodecyl-sulfate polyacrylamide gel electrophoresis
SEM	Standard error of mean
smRxr	*Sebastiscus marmoratus* retinoid X receptor
TBT	Tributyltin chloride
TMTC	Trimethyltin chloride
TPT	Tripropyltin chloride
TR	Thyroid hormone receptor
Tween 20	OptiMEM® I reduced serum medium Polysorbate 20
UAS	Upstream activation sequence
UV	Ultraviolet
VDR	Vitamin D receptor
zfRxr	*Danio rerio* Rxr

Abstract

The retinoid X receptor (RXR) is a ligand-activated transcription factor and a member of the nuclear receptor (NR) superfamily. In mammals, this receptor consists of three major subtypes, Rxra, Rxrb and RXRg, in addition to several isoforms. The receptor is diverse, and depending on isoform, ligand, and NR partner protein, RXR can regulate numerous physiological processes such as lipid metabolism and homeostasis. RXR acts both as a homodimeric transcription factor, and as a heterodimeric transcription factor dimerizing with other NRs (such as vitamin D receptor and pregnane X receptor). Exogenous ligands, such as persistent organic pollutants, have been reported to cause disruption in RXR signaling. Organotins are a class of environmental pollutants particularly prominent in marine environments that has been shown to cause endocrine disruption through binding of RXR. Atlantic cod *(Gadus morhua*), similarly to several other teleosts, has four identified Rxr subtypes, including gmRxra, gmRxrb1, gmRxrb2 and gmRxrg. gmRxrb1 and gmRxrg have previously been cloned from Atlantic cod and used in establishing luciferase reporter gene assays for ligand-activation analyses. In this thesis, the two remaining Rxr subtypes, i.e. Rxra and gmRxrb2 were cloned, and luciferase reporter gene assays were established to assess and compare the transactivation of all the Atlantic cod gmRxr subtypes to 9-cis RA and five different organotins (tributyltin, tripropyltin, fentin chloride, fentin hydroxide and trimethyltin). During gene cloning, a gmRxrb2 splice variant was identified, and further included in establishing the luciferase reporter gene assay. gmRxra and gmRxrg were transactivated by both 9-cis RA and most organotins, whilst gmRxrb2 and gmRxrb1 were not transactivated by neither compound. TBT was the most potent of the organotins, and gmRxra demonstrated the highest activation among the subtypes. Interestingly, the gmRxrb2 splice variant that lacked a stretch of 14 amino acids in helix 7 in the ligand binding domain was activated in a similar manner as gmRxra, suggesting that the removal of these amino acids is crucial for the ability of gmRrxrb to be activated. Atlantic cod is an economically and ecologically important species in the North Atlantic, but knowledge on how organotins can modulate the Rxr signaling binding in this species is limited. The observed potential of organotins to transactivate Atlantic cod Rxr subtypes could indicate that exposure to organotins can cause adverse health effects in this species, and possibly also in other teleosts.

1. Introduction

1.1 Environmental pollutants

Environmental pollutants are anthropogenic compounds that can cause adverse health effects when introduced into the environment (Moldoveanu and David, 2021). These compounds can be found in water, air, and soil, depending on the emission source and the physico-chemical properties of the compound itself (van Gestel *et al.*, 2019). Examples of abundant environmental pollutants are organochlorines (e.g., lindane and PCBs), brominated flame retardants, and per- and polyfluoroalkyl substances (PFAS) (van Gestel *et al.*, 2019). Such compounds pose a risk to all living organisms (Huang *et al.*, 2020).

Environmental pollutants are typically grouped into persistent organic pollutants (POPs) and endocrine disrupting compounds (EDCs). POPs are a collective term for anthropogenic organic compounds that have been released both intentionally and unintentionally into the environment and causing adverse effects on biota, even in low concentrations (Kim *et al.*, 2019). POPs are carbon-based compounds, and their combination of physical and chemical properties give them specific characteristics, such as being stable and resistant to degradation and having long environmental half-lives, having the potential for accumulation in large quantities in organisms, and the ability to biomagnify up the food chains (Kahn *et al.*, 2021). This allows pollutants to be readily available to exert their toxicological effects. POPs have been linked to adverse effects on both human and environmental health, for instance by being associated with allergies, cancer, damage to nervous systems, and disruption of the immune system. Some POPs can also act as endocrine disruptors and therefore also negatively affect reproductive and developmental systems.

The release of POPs into the environment over several decades has led to their wide global distribution, even at locations sites far away from their usage and production sites (Hung *et al.*, 2016). In the Stockholm Convention on Persistent Organic Pollutants, which was signed in 2001, measures and restrictions were implemented with a goal of eliminating, restricting and reducing production, use, and release of POPs. Today, there are 29 chemicals listed in the Stockholm Convention (van Gestel *et al.*, 2019). Also, other regulations have been implemented which has led to a decrease of POP production, however, many compounds still persist in nature in so-called hotspots and their surrounding areas.

Endocrine disrupting compounds (EDCs) are a large class of both natural or synthetic compounds in which through environmental or developmental exposures interfere with hormone biosynthesis, metabolism, and regulation, ultimately leading to alteration of normal homeostasis and reproduction (Diamanti-Kandarakis *et al.*, 2009). EDCs include a large amount of chemicals which are used globally and are present in the environment, such as industrial solvents and their byproducts, pesticides, plastic additives, fuels, and pharmaceuticals (Diamanti-Kandarakis *et al.*, 2009). For instance, endocrine-disrupting compounds can affect and disrupt endocrine systems by mimicking hormones. This can lead to changed endocrine function, changed behavior, decreased reproduction rate, and infant mortality, ultimately posing the ability to cause population decrease and even extinction (Huang *et al.*, 2020; Kidd *et al.*, 2007).

1.2 Organic tin compounds (OTCs)

Organic tin compounds (also known as OTCs or organotins) are environmental pollutants characterized by a Sn-atom covalently bound to at least one organic substituent (for instance methyl, ethyl, butyl, propyl and phenyl) (Hoch, 2001). Organotins are among the most widely used organometallic compounds (Sunday, Alafara and Oladele, 2012). Historically, these compounds have been used in a variety of agricultural and industrial applications, for instance in anti-fouling agents, pesticides, wood preservatives, and PVC stabilizers. Organotins, especially in a trisubstituted form, such as tributyltin (TBT) have been observed to be highly toxic to marine organisms and persist degradation in marine environments (Brändli, Breedveld and Cornelissen, 2009) (Figure 1). These compounds possess both lipophilic and hydrophilic properties and are able to bioaccumulate and biomagnify in organisms (Zhang, Li and Li, 2021). However, the toxicity of organotins has yet to be fully understood. Although not yet classified as a POP, several organotins share functional properties with compounds listed in the Stockholm Convention on Persistent Organic Pollutants.

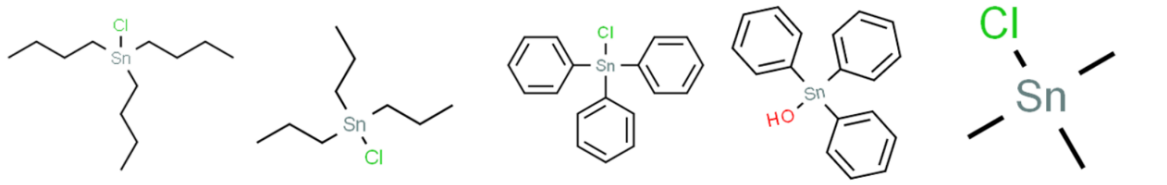

Tributyltin chloride (TBT) | Tripropyltin chloride (TPT) | Fentin chloride (FC) | Fentin hydroxide (FH) | Trimethyltin chloride (TMTC)

Figure 1: Chemical structure of five organotins used in this thesis. From left: Tributyltin chloride, tripropyltin chloride, fentin chloride, fentin hydroxide and trimethyltin chloride. These organotins can be found in marine environments and were used in this study to assess transactivation of gmRxr subtypes by organotin exposure.

Antifouling paints containing organotins, usually TBT, were implemented in the 1960s for use on ships and aquaculture installations. This was the main source of organotin release in the marine environment. In 1980, the global use of TBT containing antifouling agents was around 2-3000 tons. In 1986 in Norway, around 140 tons of organotins were used in antifouling treatment on aquaculture installations (Beyer *et al.*, 2022). TBT has been considered as one of the most toxic anthropogenic chemicals ever to be intentionally released into the environment in large amounts. TBT has received considerable attention when it comes to environmental effects and fate, especially due to its ability to function as an EDC and therefore also its potential to influence biological fitness. The widespread use of organotins has led to significant pollution worldwide, and for the most contaminated areas, often called hotspots, this contamination continues to persist (Beyer *et al.*, 2022). When TBT enters marine ecosystems, the degradation and behavior depend on factors such as pH and salinity. In normal seawater conditions, TBT typically exists as uncharged hydroxyl complexes (TBT-OH) and will therefore share similar properties as hydrophobic organic contaminants (Brändli, Breedveld and Cornelissen, 2009). In sediments that are well-oxygenated, TBT has a half-life of around 1-5 years, however, in sediments with anoxic conditions and a high organic content, the half-life can be several decades (Huang and Matzner, 2004; Langston *et al.*, 2015).

Numerous marine organisms have been affected by organotin exposure. In the early 1970s, developmental disorders in the oysters *Ostrea edulis* and *Crassosrea gigas* were observed. Similar effects were also observed in neogastropod snails, for instance dogwhelk (*Nucella lapillus*) and mud snails (*Nassarius obsoletus*). These effects were observed to be more prominent in busy coastal locations. The oysters experienced shell thickening, while female neogastropods developed tissues similar to *vas deferens* and penis-like organs (Blaber, 1970;

Matthiessen and Gibbs, 1998). This development was later linked to organotin toxicity in areas with concentrations of TBT around 2 ng/L in seawater. This irreversible disorder, which led to superimposed male genitalia production in females, was called imposex (Huang *et al.*, 2020; Smith, 1971). Imposex is a specific and dose-dependent biological effect and has been used as a biomarker for TBT pollution (Laranjeiro *et al.*, 2018). This reproductive health effect can result in unbalance of marine ecosystems, and some affected populations of marine gastropods were at a risk of extinction (Warford *et al.*, 2022). Other effects observed were growth reduction, developmental issues, increased mortality rate, induced DNA damage and reduced survival rate of hatchlings (Higuera-Ruiz and Elorza, 2011; Huang *et al.*, 2020; Widdows and Page, 1993).

After discovering the toxicity of TBT for non-target species, regulations and restrictions for its use in antifouling agents started to be developed and implemented in the 1980s. Countries included in the Oslo-Paris commissions (OSPAR) started to gradually eliminate antifouling paints containing organotins, and from around the millennium, the International Maritime Organization (IMO) initiated a worldwide removal strategy by creating the "International Convention on the Control of Harmful Antifouling systems" in 2001 (Warford *et al.*, 2022). This introduced a final deadline of a global ban of all antifouling paints containing TBT by 2008. This strategy also included a ban of vessels containing either exposed TBT or poorly sealed TBT from entering EU ports (Warford *et al.*, 2022). Due to the global ban of organotin-containing antifouling agents on ships and vessels, the contamination levels have significantly decreased in coastal waters and harbors (Pougnet *et al.*, 2014). Based on observations from monitoring of neogastropods in heavily affected areas, imposex rates are declining and health improvements have led to recovery of several snail populations worldwide (Schøyen *et al.*, 2019). However, there are still indications of production and sales of antifouling agents containing organotins in recent years, and TBT continuous to persist and is still contaminating marine environments worldwide (Paz-Villarraga, Castro and Fillmann, 2022). Hence, TBT is still considered a contaminant of emerging concern. A total recovery of imposex remains to be achieved. Several factors affect the persistence of TBT, not only the properties of the contaminant, but also poor handling and disposal of contaminated vessels and paints. Environmental factors such as a storm event can also lead to sediment disturbance, which can cause TBT desorption from the sediments to the water. Therefore, continuous monitoring is important for following global TBT pollution trends for the future (Laranjeiro *et al.*, 2018).

In Norway, the maximum tolerable risk limit of TBT polluted sediments has been set to 35 µg/kg dry weight (d.w.). However, 95 coastal sites in Norway demonstrate TBT concentration above this limit (Figure 2). Among these hotspots, the highest TBT mean concentration value measured exceeded 30 000 µg/kg d.w., while the highest concentration detected exceeded more than 100 000 µg/kg d.w. When comparing these locations to the most contaminated hotspots globally, the Norwegian TBT hotspots can be compared to the most contaminated TBT hotspots worldwide. Interestingly, the Norwegian hotspots are found in smaller harbors and port locations, whilst the hotspots in other countries are found in major ports and shipyards (as reviewed by Beyer *et al.*, 2022).

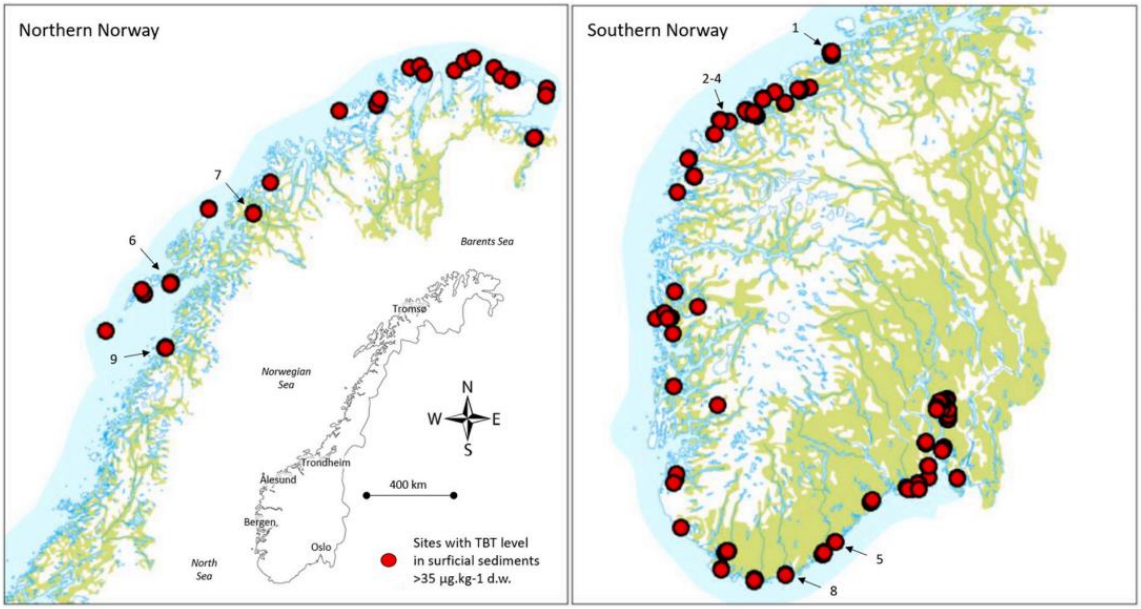

Figure 2: Map showing distribution of TBT hotspots along the Norwegian coastline. 95 coastal sites (marked with red dots) indicate measured TBT concentration in sediments above the maximum tolerable risk limit of 35 µg/kg d.w. The numbers (1-9) indicate the top nine locations with the highest mean sediment concentrations of TBT. Illustration adapted from Beyer *et al.* (2022).

1.2.1 Organotin toxicity

Initial studies regarding the mode of action (MoA) of TBT-mediated toxicity focused on inhibitory and modulative interactions to metabolic pathways and detoxifying enzyme systems, such as the cytochrome P450. This MoA was based on inhibition of CYP19A (aromatase) resulting in a shift in female androgen-estrogen balance, which was believed to be the cause of development of male genital organs (Bettin, Oehlmann and Stroben, 1996). Organotins have been reported to inhibit aromatase CYP19A activity in female zebrafish (*Danio rerio*), causing

increase in androgen levels and ultimately resulting in masculinization (Cheshenko *et al.*, 2008). However, the CYP19A aromatase enzymes, or homologues, are yet to be identified in mollusks, or outside of bilaterian animals in general, which is why the hypothesis of organotin-induced aromatase-like inhibition causing neogastropod imposex has been dismissed in recent years (Fodor *et al.*, 2020).

Recent studies have narrowed the TBT-induced imposex to involvement of nuclear receptors (NRs), such as the retinoid X receptor (RXR), and the condition is believed to be developed through organotin-mediated disruption of RXR signaling (Huang *et al.*, 2020). This MoA hypothesis can be reinforced as imposex also occurs when female gastropods are solely exposed to 9-cis retinoic acid, an endogenous RXR ligand (Castro *et al.*, 2007). The RXR signaling pathway has also been linked to oyster shell thickening in recent studies. Organotin-induced imposex through RXR disruption in marine organisms is a hypothesis gaining evidence.

1.3 Nuclear receptors

Nuclear receptors (NRs) are a superfamily of ligand-activated transcription factors that regulate gene expression, and therefore provide a direct link between signaling molecules controlling processes such as homeostasis, development, reproduction, metabolism, and transcriptional responses in an organism (Huang *et al.*, 2020; Laudet, 2006). NRs are found widely in animals, including humans, other chordates, and insects. The mechanism of the ligand-dependent action of NRs is initiated when the activated receptors translocate into the nucleus where it binds to DNA-specific sites. After binding to DNA, it can regulate target gene expression, which can start a variety of cellular processes (Ishigami-Yuasa and Kagechika, 2020). In general, NRs bind small lipophilic ligands, for instance steroids, retinoids, thyroid hormones, and lipids that are transported across the cell membrane (Rastinejad *et al.*, 2013; Weikum, Liu and Ortlund, 2018).

NRs have classically been separated into two functional classes. Class I NRs form homodimers and include RXRs and the steroid hormone receptors such as estrogen receptors (ERs) and progesterone receptor (PRs). Class II function as heterodimers with RXR, such as retinoic acid receptors (RARs), peroxisome proliferator-activated receptors (PPARs) and thyroid hormone receptors (TRs) (Beinsteiner *et al.*, 2022). Even though NRs are structurally similar, the variations in the ligand binding domain and the DNA-binding domain are responsible for the diverse regulation of cellular processes. NRs are activated by endogenous compounds, for

instance hormones, and are therefore susceptible to interference by endocrine disruptive compounds (Huang *et al.*, 2020). Therefore, NRs have been widely used as molecular targets in drug discovery (Yang, Li and Li, 2014).

Based on their nucleotide sequences, NRs are organized in seven subfamilies, named NR0-NR6 (Weikum, Liu and Ortlund, 2018) (Figure 3). The NR0 contains all known receptors lacking the typical NR domains. Recent studies have also discovered an ancient NR subfamily, named NR7, which can give information on the initial steps of NR diversification (Beinsteiner *et al.*, 2022). NR1 consists of receptors such as RAR, TR, and PPAR, and is considered the largest subfamily. NR2 is the second largest subfamily, which includes RXR. RXR form heterodimers with members of the NR1 subfamily.

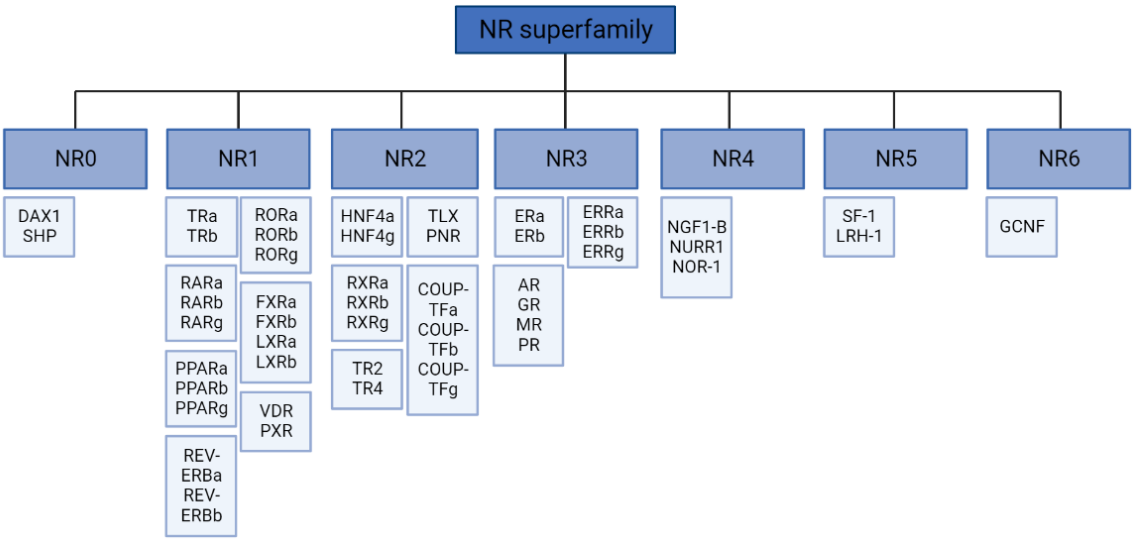

Figure 3: The NR superfamily. An overview of the seven NR subfamilies detected in human RXR, with the individual NRs divided into groups within the subfamilies (Weikum, Liu and Ortlund, 2018). Illustration made with Biorender.

1.4 Retinoid X receptor (RXR)

1.4.1 Subtypes and roles

Retinoid X receptors (RXRs) are important members of the NR2 superfamily. There are three known RXR subtypes derived from three distinct genes, encoding the RXR alpha (RXRa), RXR beta (RXRb), and RXR gamma (RXRg) proteins. RXRs are involved in numerous

physiological processes due to their variation in subtypes, but also due to being heterodimerization partners of many other NRs (Laudet, 2006; Maire *et al.*, 2022; Watanabe and Kakuta, 2018). Unlike the NR1 family of NRs, RXRs can also bind to DNA as monomers or homodimers (Li *et al.*, 2004). Its central role makes also RXRs a potential therapeutic target for treatment of diseases, for instance metabolic diseases or cancer (Dawson and Xia, 2012).

Some RXR heterodimers are permissive, meaning they become transcriptionally active only in the presence of an RXR selective ligand or NR partner ligands such as the PPAR:RXR heterodimer (Figure 4). 9-cis retinoic acid is an example of a potent endogenous agonist for RXRs (Watanabe and Kakuta, 2018). Non-permissive heterodimers do not respond to an RXR-selective ligand alone but activate transcription by synergizing with partner agonists (Pérez *et al.*, 2012). An RXR heterodimer with the thyroid hormone receptor (TR) is an example of a non-permissive heterodimer (TR:RXR) (Kojetin *et al.*, 2015). The ability to heterodimerize with a wide range of nuclear receptors gives RXR a unique role in the nuclear receptor superfamily. For instance, PPAR:RXR is an extensive signaling mediator for PPAR ligands, but also for the RXR ligand 9-cis RA (Ijpenberg *et al.*, 2004).

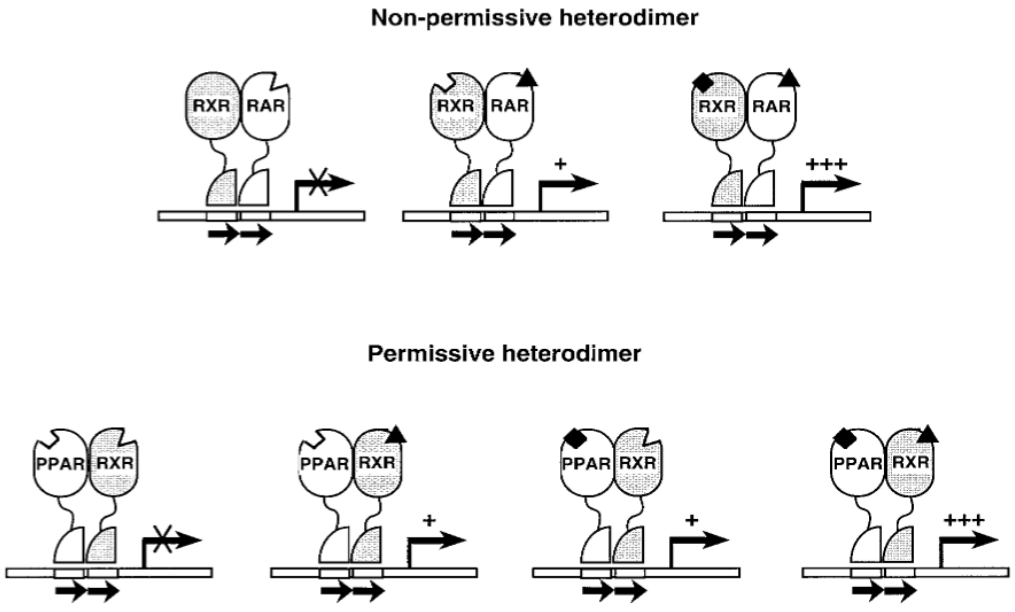

Figure 4: RXR act as a non-permissive and permissive heterodimer. The figure shows a non-permissive heterodimer of RXR and RAR and a permissive heterodimer between RXR and PPAR. "X" indicates no transcriptional activation, "+" indicates transcriptional activation of target gene, and "+++" indicates synergistical transcriptional activation of target gene. Illustration from Aranda and Pascual (2001).

1.4.2 RXR protein structure

RXRs share similar protein structure with other members of the NR superfamily. However, there are some differences between the subtypes RXRa, RXRb and RXRg making them able to diversely interact with ligands and regulate gene expression. This also leads to a diverse involvement of the subtypes in physiological processes, such as cell growth and homeostasis (Chen *et al.*, 2018).

The characteristic protein structure consists of conserved regions with specific functional domains (Pawlak, Lefebvre and Staels, 2012) (Figure 5). The domains are the non-conserved N-terminal domain (A/B region), the highly conserved DNA-binding domain (DBD) (C region), the non-conserved hinge region (D region), a moderate conserved ligand binding domain (LBD) (E region), and the highly diverse C-terminal (F region) (Laudet, 2006). The DBD and LBD are connected by a flexible hinge, which is central for selection of DNA binding sites. This hinge acts as a regulatory region of target genes (Beinsteiner *et al.*, 2022).

The LBD has a key role in ligand mediated RXR activity, such as ligand interactions and transcriptional activation (Jin and Li, 2010; Sharma *et al.*, 2022). LBD binding to ligands is followed by recruitment of transcriptional coregulators which then triggers induction or repression of target genes. LBP is the least conserved region in the LBD and contributes to ligand binding specificity and affinity. In addition, it provides RXR greater flexibility due to its "plastic nature" and variation in size and shape, which makes the receptor susceptible to binding to a variety of ligands. The LBP also has a hydrophobic nature, which makes it able to interact with lipid soluble ligands (Jin and Li, 2010).

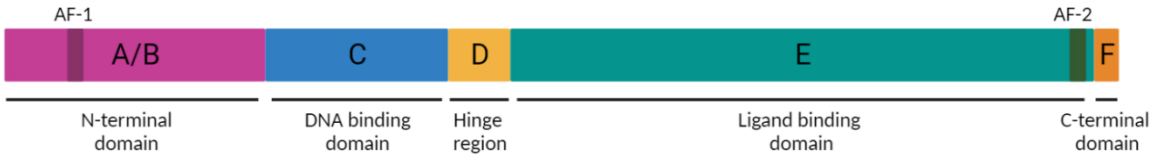

Figure 5: The five functional domains of RXR, including activation function 1 and 2 (AF-1 and AF-2). Illustration created in BioRender.

1.4.3 RXR endogenous ligands

Despite of RXRs ubiquitous presence and central position in cellular signaling, RXR endogenous ligands and physiological functions remain to be fully elucidated, and the matter is still widely debated. Initial studies indicated 9-cis-retinoic acid (9-cis RA) as a natural endogenous ligand for all RXR subtypes (Figure 6). 9-cis retinoic acid is a vitamin A-derived metabolite containing a carboxylic head group and a long aliphatic chain (Maire *et al.*, 2022). This retinoid is involved in several physiological processes and its pleiotropic effects are mediated through direct binding to both RXRs and RARs. Hormone binding to RXR:RAR LBD results in conformational changes that affect helix H12, which has an important role in transcriptional activation, located in the C-terminal part (Egea *et al.*, 2001).

9-cis retinoic acid has been widely used as a model-ligand in RXR research due to its high affinity binding. Even though RAR also binds 9-cis RA, it also binds all-trans RA, whilst RXR solely binds 9-cis RA (Egea 2001; Tate *et al.*, 1994). Recent studies propose that several fatty acids and retinoic acid analogs might be endogenous ligands of mammalian RXRs, for instance phytanic acid (PA) and the unsaturated fatty acid docosahexaenoic acid (DHA) (Figure 6). However, these ligands have also been found to have a low affinity to RXR and weak transactivation capacity due to being tissue specific, which raises the question of them being true endogenous ligands (Dawson and Xia, 2012; Maire *et al.*, 2022).

1.4.4 RXR exogenous ligands

In addition to organotins, there are other known RXR exogenous ligands such as the synthetic RXR agonist bexarotene (LGD1069). Bexarotene has been approved as an anticancer treatment for cutaneous T cell lymphoma (Tanaka and De Luca, 2009). When interacting with RXRa, this agonist has shown to exert neurological effects, such as inducing apoptosis in T-cell lymphoma cells (Querfeld *et al.*, 2006). Bexarotene has also been reported to selectively bind to RXRa/b/g in humans in comparison to RAR (Boehm *et al.*, 1995; as reviewed by Sharma *et al.*, 2022).

LG100268 is a structural analog of bexarotene and a synthetic RXR agonist with high potency and selectivity for RXR. Therefore, it is often used for studying RXR signaling pathways. This compound has been reported to transactivate RXR at concentration tenfolds lower than that of 9-cis RA (Boehm *et al.*, 1995). LG100268 has also been shown to activate heterodimers such as RXR/LXR and RXR/PPAR (Cesario *et al.*, 2001). There has also been recent observation of LG100268 plausibly causing endocrine disruption in the fish *Paralichthys olivaceus* through

activation of Rxr[1], where the percentage of male fish fry increased from 50% to 71.4% after exposure (Zou *et al.*, 2023).

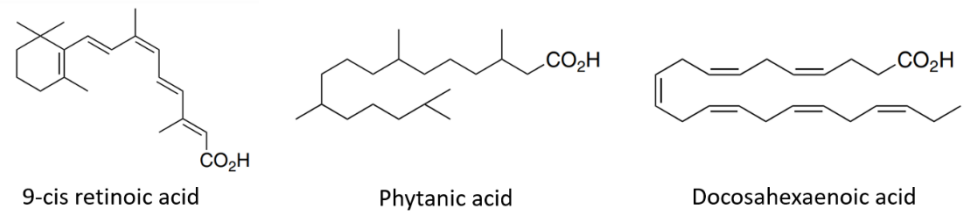

Figure 6: Putative endogenous and exogenous ligands of RXR. 9-cis retinoic acid was used in this study to assess transactivation of gmRxr. Illustration adapted from Dawson and Xia (2012).

1.5 Atlantic cod

Atlantic cod (*Gadus morhua*) is a teleost distributed both offshore and in coastal areas across the North Atlantic Ocean (Johansen *et al.*, 2009). The species is usually located between 50-400 meters, however its range is from right below surface levels to approximately 600 meters, whereas the juveniles are often located in the upper 50 meters (Hansen *et al.*, 2016). Atlantic cod has been recognized with evolutionary divergence of ecotypes. In Northern Norway, Iceland and Canada there is a migratory form, which spawn in shallow and coastal areas, whilst using the open ocean for feeding. On the other hand, there are populations in Southern Norway, Iceland and Canada that remain in fjords throughout their entire lifecycle (Kristensen *et al.*, 2021; Wroblewski, Neis and Gosse, 2005).

Atlantic cod is considered a key species and dominant top predator and can therefore affect the trophic structure and function of marine ecosystems (Östman *et al.*, 2016). Several natural cod populations have previously been threatened by environmental changes and overexploitation, and some populations are yet to recover. After several cod populations collapsed in the early 1990s across Atlantic Canada due to overfishing, there was a change in fish diversity which caused ecosystem instability (Ellingsen *et al.*, 2015). In coastal Skagerrak, the decline of cod populations has been linked to a trophic cascade causing degradation of seagrass and seaweed

[1] In this thesis, the nomenclature where proteins from mammals are written in all capitals ("HGNC Guidelines,") was followed, whereas short names of fish proteins are written with only the first letter in capital (Nathan Dunn, 2019).

habitats, which are areas important for feed and shelter for several invertebrates and fish (Kristensen *et al.* 2021; Östman *et al.*, 2016).

Several measures have been implemented to promote the recovery of Atlantic cod populations, however most of these measures have been characterized as inefficient (Sguotti *et al.*, 2018). Even though some recovery has been observed, Atlantic cod populations are still threatened. This could be due to a combination of multiple drivers that cause pressure on spawning and full recovery, such as ocean warming, fishing pressure, high natural mortality by predation and environmental pollutants (Link *et al.*, 2009; Sguotti *et al.*, 2018). Another notable cause preventing cod population recovery could be due to Atlantic cod being important prey for species such as grey seals (*Halichoerus grypus*), which causes high natural mortality (Hammill *et al.*, 2014). Due to its wide distribution and economical and ecological importance, Atlantic cod has been used as a bioindicator species for environmental monitoring studies of Norwegian coastal areas and fjords since the 1980s by the Joint Assessment and Monitoring Program (JAMP) (Søfteland, Holen and Olsvik, 2010). The aim of this monitoring is to detect the possible effects environmental pollutants can have on Atlantic cod, and potentially other marine teleost species.

The Atlantic cod genome sequence was published by Star *et al.* in 2011. This data can give insight into how Atlantic cod responds to anthropogenic chemicals on a genomic scale (Eide *et al.*, 2018; Karlsen, Puntervoll and Goksøyr, 2012).

1.5.1 Atlantic cod Rxr

The characteristics of Rxr in Atlantic cod and most teleost species in general is an area of limited knowledge. However, Rxr in zebrafish (*Danio rerio*) are described to some extent (Cunha *et al.*, 2017; Tallafuss *et al.*, 2006). Rxr in teleost species usually possess Rxra, two Rxrb (Rxrb1 and Rxrb2), and gmRxrg subtypes, while in most mammalian species only one of each Rxra, Rxrb, and Rxrg subtype has been identified (Tallafuss *et al.*, 2006; Waxman and Yelon, 2007). The variation of Rxr isoforms present in teleost species is believed to be caused by teleost specific whole genome events, or tandem duplication events of genes encoding Rxr, giving the teleost Rxr the possibility to obtain new functional properties. Eide *et al.* (2018) published a genomic mining study where the four gmRxr isoforms were identified as part of mapping all members of the NR superfamily in the Atlantic cod genome. Borge (2021) performed a tissue specific expression profile of the four known Rxr subtypes of Atlantic cod (gmRxra, gmRxrb2,

gmRxrb2 and gmRxrg) (Appendix Figure A), and cloned and integrated gmRxrb1 and gmRxrg into a luciferase-based reporter gene assay to study their activation by 9-cis RA and organotins (TBT, TPT, FC, FH and TMTC) *in vitro*. In this study, it was observed that 9-cis RA activated gmRxrg, but not gmRxrb1. The same pattern was observed with most of the organotins tested.

1.6 Aim of the study

Even though monitoring programs indicate that organotin levels in the environment are declining, there are still observations of organotin-mediated effects in marine organisms, as well as organotin concentrations in hotspots along the Norwegian coast are among the highest observed globally. Furthermore, studies regarding organotin-mediated effects on cold-water marine teleosts are limited. It is therefore a need to assess the possibility of organotins to activate gmRxr at low concentration (nM-µM) and obtain knowledge on the potential adverse effects these compounds may have on marine teleosts when modulating the Rxr signaling pathway.

The aim of this study was therefore to study Rxr nuclear receptors in Atlantic cod (gmRxr) with regard to their ligand activation capabilities to a known endogenous RXR ligand, i.e. 9-cis RA, and several organotins as potential exogenous ligands. The subgoals for this thesis are listed below.

I. Clone and sequence the *gmrxra* and *gmrxrb2* (hinge-region and LBD) subtypes from Atlantic cod tissue.
II. Establish a luciferase-based *in vitro* reporter gene assay for assessing ligand-binding and transcriptional activation of gmRxra and gmRxrb2.
III. Conduct a comparative transactivation study of all gmRxr subtypes by using 9-cis RA and a selected set of organotins (TBT, TPT, FC, FH and TMTC) and comparing potencies and efficacies among the different ligands and receptors.

2. Materials

2.1 Reagents and chemicals

Table 1: Reagents and chemicals used

Name	Chemical formula	Supplier
10X loading buffer	-	TaKaRa
2-log DNA ladder	-	New England
2-b-Mercaptoethanol	$HSCH_2CH2OH$	Aldrich
2-2-nitrofenyl-b-D-galactopyranoside	$C_{12}H_{15}NO_8$	Sigma-Aldrich
3-(4.5-Dimethyliazol-2-yl)-2.5-Diphenyltetrazoliumbromide	$C_{25}H_{20}BrN_3O_2S$	Merck
5-Carboxyfluorescein diacetate, Acetoxymethyl ester (5-CFDA-AM)	$C_{28}H_{20}O_1$	Thermo Fisher Scientific
Acetic acid	CH_3COOH	Sigma-Aldrich
Acrylamide-Bis	-	Bio-Rad
Adenosin 5’ triphosphate disodium salt hydrate (ATP)	C_3H_5NO	Sigma-Aldrich
Agar-agar	-	Merck
Agarose	-	Sigma-Aldrich
Ammonium persulfate	$(NH_4)_2S_2O_8$	Sigma-Aldrich
Ampicillin sodium salt	$C_{16}H_{18}N_3NaO_4S$	Sigma-Aldrich
Betain	$C_5H_{11}NO_2$	Sigma-Aldrich
Boric acid	H_3BO_3	Merck
Bovine serum albumin	-	Sigma-Aldrich
Co-enzyme A	-	Thermo Fisher
CHAPS	$C_{32}H_{58}N_2O_7S$	Thermo Fisher
Dimethyl sulfoxide (DMSO)	C_2H_6OS	Sigma-Aldrich
Disodiumhydrogenphosphate	Na_2HPO_4	Sigma-Aldrich
DL-Dithiothreitol (DTT)	$HSCH_2CH(OH)CH(OH)CH_2SH$	Sigma-Aldrich
D-luciferin sodium salt	$C_{11}H_8N_2O_3S_2$	Biosynth
Dulbecco’s modified Eagle’s medium (phenol red)	-	Sigma-Aldrich
Dulbecco’s modified Eagle’s medium (w/o phenol red)	-	Sigma-Aldrich
Erythrosin-B	$C_{20}H_8I_4O_5$	Sigma-Aldrich
Ethanol	C_2H_5OH	Sigma-Aldrich
Ethidium bromide	$C_{21}H_{20}BrN_3$	Sigma-Aldrich
Ethylene glycol-bis(b-aminoethyl ether)-N´,N´,N´,N´-tetraacetic acid (EGTA)	$C_{14}H_{24}N_2O_{10}$	Sigma-Aldrich

Ethylenediaminetetraacetic acid	$C_{10}H_{16}N_2O$	Sigma-Aldrich
Fetal bovine serum (FBS)	-	Sigma-Aldrich
Galactose	-	Sigma-Aldrich
GelRed	-	Biotium
Glycerol	$C_3H_8O_3$	Sigma-Aldrich
Isopropanol	C_3H_8O	Kemetyl
L-glutamine	$C_5H_{10}N_2O_3$	Sigma-Aldrich
L-a-Phosphatidylchlorine	$C_{44}H_{88}NO_8P$	Sigma-Aldrich
Magnesium carbonate hydroxide pentahydrate	$(MgCO_3)4 \bullet Mg(OH)_2 \bullet 5H_2O$	Sigma-Aldrich
Magnesium chloride hexahydrate	$Mg(CL_2) \bullet 6H_2O$	Sigma-Aldrich
Magnesium sulfate heptahydrate	$H_{14}MgO_{11}S$	Sigma-Aldrich
Methanol	CH_3OH	Sigma-Aldrich
Monosodium phosphate	NaH_2PO_4	Sigma-Aldrich
o-Nitrophenyl b-d-galactopyranoside (ONPG)	$C_{12}H_{15}NO_8$	Sigma-Aldrich
OPTI-MEM®	-	Gibco
Polysorbate 20 (Tween 20)	$C_{58}H_{114}O_{26}$	Thermo Fisher
Resazurin sodium salt	$C_{12}H_6NNaO_4$	Sigma-Aldrich
Penicillin-Streptomycin	-	Sigma-Aldrich
Phosphate-buffered saline (PBS)	$Cl_2H_3K_2Na_3O_8P_2$	Sigma-Aldrich
Phenylmethylsulfonyl fluoride (PMSF)	$C_7H_7FO_2S$	Sigma-Aldrich
Potassium chloride	KCl	Sigma-Aldrich
Sodium chloride	NaCl	Merck
Sodium dodecyl sulfate (SDS)	$NaC1_2H_{25}SO_4$	Merck
Sodium pyruvate	$C_3H_3NaO_3$	Sigma-Aldrich
Trans IT®-LT1	-	Mirus Bio LLC
Tricine	$C_6H_{13}NO_5$	Sigma-Aldrich
Tris-hydrochloric acid	HCl	Sigma-Aldrich
Triton^{TM} X-100	-	Sigma-Aldrich
Trypsine-EDTA	-	Sigma-Aldrich
Tryptone	-	Merck
Yeast extract	-	Sigma-Aldrich

2.2 Plasmids

Table 2: Plasmids used

Plasmid name	Method used in
Mh(100)x4tk luc	Luciferase gene reporter assay
pCMV-b-gal	Luciferase gene reporter assay
pSC-B	Vector for blunt cloning

pSC-B-Rxra	pCMX-GAL4-Rxra/b1/b2/g construction
pSC-B-Rxrb1	pCMX-GAL4-Rxra/b1/b2/g construction
pSC-B-Rxrb2	pCMX-GAL4-Rxra/b1/b2/g construction
pSC-B-Rxrg	pCMX-GAL4-Rxra/b1/b2/g construction
pCMX-GAL4-LBD	pCMX-GAL4-Rxra/b1/b2/g construction
pCMX-GAL4-Rxra	Luciferase gene reporter assay
pCMX-GAL4-Rxrb1	Luciferase gene reporter assay
pCMX-GAL4-Rxrb2	Luciferase gene reporter assay
pCMX-GAL4-Rxrg	Luciferase gene reporter assay

2.3 Enzymes

Table 3: Enzymes used

Name of enzyme	Supplier
Big dye terminator	Applied biosystems
DreamTaq green DNA polymerase	Life Technologies
Phusion Hot start II DNA polymerase	Thermo Fisher Scientifics
RNase H	Invitrogen
RNaseOUT^{TM} Recombinant RNase inhibitor	Invitrogen
SuperScript® IV Reverse Transcriptase	Invitrogen
Shrimp alkaline phosphatase (SAP)	Affymetric
EcoRI – Restriction enzyme	Takara
NheI – Restriction enzyme	Takara
T4 DNA ligase	Takara

2.4 Primers

Table 4: Primers used

ID	Name	Sequence 5'-3'
MT2044	gmRxra fwd.	GTAGTTGAATTCTTACACGCAGCCGTTCAGGA
MT2046	gmRxra rev.	ttgacaGCTAGCCTATGTCATCTGATGTGGTGC
MT2048	gmRxrb2 fwd.	GTAGTTGAATTCGAACGTCAGAGATCGGTGCA
MT2049	gmRxrb2 rev.	ttaataGCTAGCCTATGGGAGCTGGTGCGGGG
MT2041	pSC-B fwd.	ATTAACCCTCACTAAAGGGA
MT2042	pSC-B rev.	TAATACGACTCACTATAGGG
MT2281	gmRxr mid.	AGCTGTTCacgCTGGTGGAGTG
MT1077	pCMX fwd.	TGCCGTCACAGATAGATTGG
MT1279	pCMX rev.	AATCTCTGTAGGTAGTTTGTCCA
MT1383	GAL4 fwd.	ATGAAGCTACTGTCTTCTATCG

MT2066	GAL4 rev.	CGATACAGTCAACTGTCTTTGAC

2.5 Cell lines

Table 5: Cell lines used

Name of cell line	Domain	Supplier
StrataClone Solo Pack Competent Cells	Prokaryote	Agilent
StrataClone "Mix&Go" Competent Cells	Prokaryote	Agilent
COS-7	Eukaryote	(Gluzman, 1981)

2.6 Growth medium

Table 6: Freezing- and cultivation medium for COS-7 cell line

Component	Concentration
Dubecco's modified Eagle's medium DMEM (with and w/o phenol red)	1 X
Fetal bovine serum (charcoal stripped for DMEM w/o phenol red)	10%
Sodium Pyruvate	1 mM
L-glutamine	200 mM
Penicillin-Streptomycin	1 U/mL
DMSO	5%

Table 7: Reagents for lysogeny broth medium (LB-medium)

Component	LB-medium	LB-agar
Tryptone	10 g/L	10 g/L
NaCl	10 g/L	10 g/L
Yeast extract	5 g/L	5 g/L
Agar-agar	-	15 g/L
Ampicillin*	-	100 mg/L
ddH_2O	-	-

*Added post autoclavation

2.7 Buffers and solutions

2.7.1 Agarose gel

Table 8: Agarose gel

Component	Concentration
TAE-buffer	1 X
Agarose	0.75%
GelRed	0.0014%

Table 9: TAE-buffer

Component	Concentration
EDTA	1 mM
Tris	40 mM
Acetic acid	20 mM
ddH_2O	-

2.7.2 Luciferase gene reporter assay

Table 10: Cell lysis buffer

Component	Concentration
Tris pH 7.8	25 mM
Glycerol	15%
CHAPS	2%
BSA	1%
L-a-Phosphatidylcholine	1%

Table 11: Cell lysis reagent solution

Component	Concentration
Cell lysis buffer	1 X
EGTA	4 mM
DDT	1 mM
MgCL2	8 mM
PMSF	0.4 mM

Table 12: 4X Luciferase base buffer

Component	Concentration
Tricine	80 mM
$(MgCO_3)4*Mg(OH)_2*5H_2O$	4.28 mM
Na_2EDTA	0.4 mM
$MgCl_2$	10.68 mM

Table 13: Luciferase reaction solution

Component	Concentration
Luciferase base buffer	1 X
MQ-H2O	-
DTT	5 mM
ATP	0.5 mM
Coenzyme A*	0.2 mM
D-luciferin*	0.5 mM

* Added right before use

Table 14: b-galactosidase buffer (10X)

Component	Concentration
Na_2HPO_4	60 mM
NaH_2PO_4	40 mM
KCl	10 mM
$MgSO_4*7H_2O$	1m M

Table 15: b-galactosidase reaction

Component	Concentration
b-galactosidase buffer	1X
DTT	5.3 mM
ONPG	8.6 mM

Table 16: Ligands used in luciferase gene reporter assay with supplier and CAS number

Name	Supplier	CAS-number
9-cis-retinoic acid	Sigma-Aldrich	5300-03-8
Tributyltin chloride	Sigma-Aldrich	1461-22-9
Tripropyltin chloride	Sigma-Aldrich	76-87-9
Fentin hydroxide	Supleco	76-87-9
Fentin chloride	Sigma-Aldrich	639-58-7
Trimethyltin chloride	Sigma-Aldrich	1066-45-1

2.7.3 Cell viability and cytotoxicity assay

Table 17: L-15/ex A

Component	Conc.
NaCl	80.0 g
KCl	4.0 g
$MgSO_4 \bullet 7H_2O$	2.0 g
$MgCl_2 \bullet 6H_2O$	2.0 g
ddH_2O	600 mL

Table 18: L-15/ex B

Component	Conc.
$CaCl_2$	1.4 g
MQH_2O	100 mL

Table 19: L-15/ex C

Component	Conc.
Na_2HPO_4	1.9 g
KH_2PO_4	0.6 g
MQH_2O	300 mL

Table 20: Cell viability solution

Component	Concentration
ddH2O	500 mL
L-15/ex solution A	34 mL
L-15/ex solution B	6 mL
L-15/ex solution C	17 mL
Galactose	0.8 mg/mL
Pyruvate	0.5 mg/mL
Resazurin	0.03 mg/mL
CFDA-AM	0.001 mg/mL

2.7.4 Western blot assay

Table 21: Components and volumes for one 12% SDS-page

Component	12% Running gel	Stacking gel
ddH_2O	2.49 mL	2.27 mL
30% Acrylamide-Bis	3.0 mL	0.65 mL
1.5 M Tris pH 8.8	1.9 mL	-

0.5 M Tris pH 6.8	-	1.0 mL
20% SDS	37.5 µL	20.0 µL
10% APS	75.0 µL	40.0 µL
TEMED	3.0 µL	4.0 µL

Table 22: 5X sample buffer

Component	Concentration
Tris HCl pH 6.8	250 mM
SDS	10%
Glycerol	30%
2-b-mercaptoethanol	5%
Bromophenolblue	0.02%

Table 23: Lysis buffer

Component	Concentration
5X sample buffer	2X
10X PBS pH 7.4	1X
100 X Protease	1X
inhibitor	
ddH_2O	-

Table 24: 10X Tris-buffered saline (TBS) pH 7.5

Component	Concentration
Tris base	24 g
NaCl	88 g
MQH_2O	900 mL
32-N-HCl	pH adjustment

Table 25: 1X TGS running buffer

Component	Concentration
Glycine	192 mM
Tris base	25 mM
SDS	0.1%

Table 26: 0.05% TBS-Tween (TBST)

Component	Concentration
10XTBS	0.5 X
Tween 20	0.05%
MQH2O	-

Table 27: 10X Tris-glycine (TG) buffer

Component	Concentration
Tris base	30.3 g
Glycine	14.4 g
MQH_2O	-

Table 28: 1X Transfer buffer (TB)

Component	Concentration
10X TG buffer	1 X
Methanol	2 X
ddH_2O	-

Table 29: Blocking solution with 7% milk

Component	Concentration
Powder milk	3.5 g
TBS-Tween	50 mL

Table 30: Primary and secondary antibodies

Antibody	Supplier
Anti-GAL4-DBD mouse monoclonal	Santa Cruz
Horseradish peroxidase linked antibody sheep Anti-mouse IgG, polyclonal	GE Healthcare
Anti b-actin monoclonal	Abcam

2.8 Kits

Table 31: List of commercial kits used, supplier and application

Name	Supplier	Application
BigDye Terminator v3.1 cycle sequencing kit	Thermo Scientific	Sanger sequencing
DreamTaq green DNA polymerase kit	Thermo Scientific	Colony PCR
NucleoBond® PC 100 plasmid purification kit	Macherey-Nagel	Plasmid purification, midiprep
NucleoSpin® plasmid purification kit	Machery-Nagel	Plasmid purification, miniprep
Phusion Hot Start II DNA polymerase kit	Thermo Scientific	PCR amplification of gmRxr from cDNA
StrataClone Blunt PCR cloning kit	Agilent	Blunt cloning into pSC-B
SuperScript® IV Reverse Transcriptase kit	Invitrogen	cDNA synthesis
T4 DNA-ligase kit	Takara	Ligate gmRxr and pCMX
SuperSignalTM West Pico PLUS Chemiluminescent Substrate kit	Thermo Scientific	Verification of protein expression in COS-7 cells
ZymoCleanTM Gel DNA Recovery kit	ZYMO Research	DNA purification

2.9 Instruments

Table 32: Instruments used

Name	Supplier	Application
Buerker hemocytometer	Marienfield	Cell counting
C1000™ Thermal Cycler	Bio-Rad	PCR amplification
ChemiDoc™ XRS+system	Thermo Scientific	Agarose gel imaging
Heraeus pico 21		Centrifugation
DM IL inverted microscope	Leica	Cell counting
Enspire™ 2300 Multilabel Reader	PerkinElmer	Reading
GD100	Grant	Heat-shocking
Heraeus multifuge X3R	Thermo Scientific	Centrifugation
HS 501 Digital	IKA®-Werle	Shaker
MilliQ A10 advantage	Merck	MQH_2O dispenser
MP220	Bergman	Shaker
Nanodrop 1000	Thermo Scientific	Concentrations of RNA, cDNA and DNA
PowerPacTM HC	Bio-Rad	Electric power to electrophoresis
Multitron standard shaking incubator	Infors HT	Cell cultivation incubation
Ultrospec 10 cell density meter	Amersham Biosciences	Culture density
UV-transiluminator	UVP	Agarose gel extraction
Thermomixer compact	Eppendorf	Heat-block
Panasonic mco-170aicuv-pe	Lab-tec	Incubation of COS7-cells with CO2
Termarks incubator	Termarks	Incubator for transfected colonies
CleanAir EuroFlow Class II biosafety cabinet	Baker	Sterilized workplace for COS7-cell handling

2.10 Software

Table 33: List of software used, including provider and application

Name	Provider	Application
BioRender 2023	BioRender®	Figure preparation
Clustal Omega	EMBL-EBI	Multiple sequence alignment
JalView 2.11.2.0		Visualization of sequence alignments
UniProt	EMBL-EBI and PIR	Genome browser
GraphPad 9.5.1	GraphPad software	Figures and statistics
SnapGene 5.3	Biotech	Primer design and cloning simulations
Word 2020	Microsoft	Thesis writing
Excel 2020	Microsoft	Assay calculations
PowerPoint 2020	Microsoft	Figure making

3. Methods

3.1 Experimental outline

Several molecular biology methods, including some bioinformatical analyses, were performed throughout this thesis. Figure 7 indicates an overview of the experimental outline, where the major approaches are indicated with darker coloring.

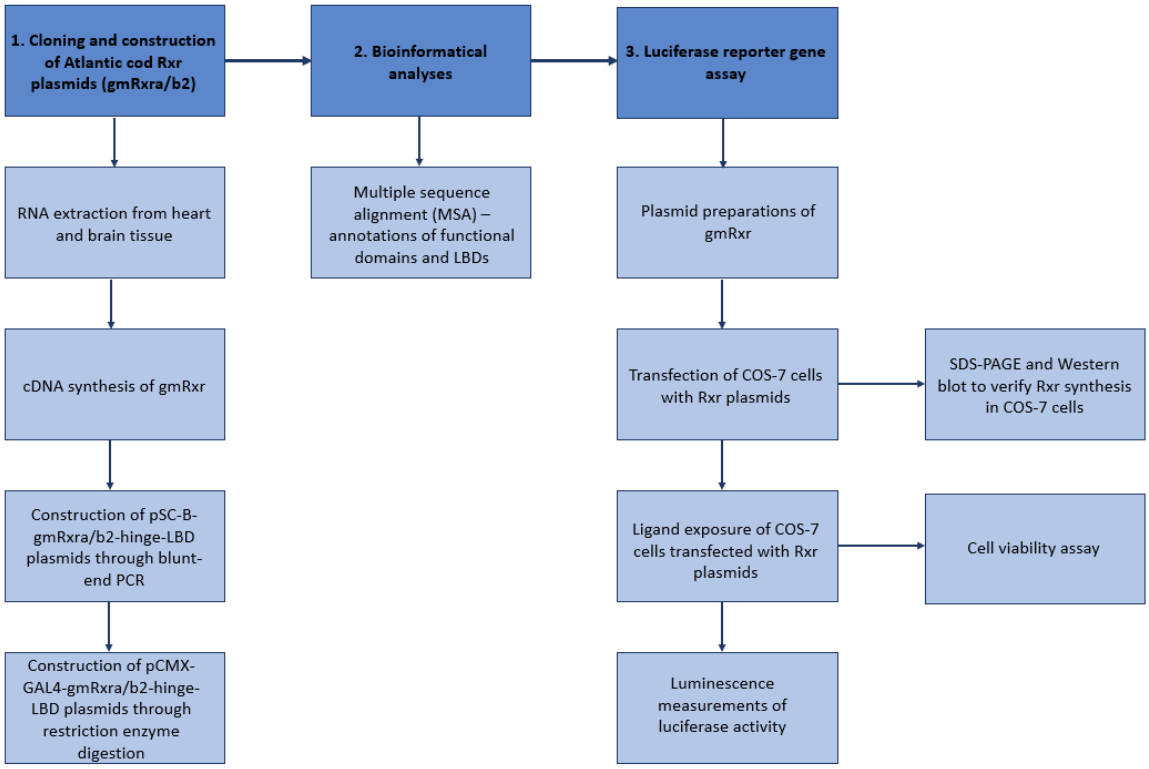

Figure 7: Experimental outline of this study. RNA was extracted from Atlantic cod (Gadus morhua) heart and brain tissue, followed by cDNA synthesis. The cDNA samples were used to clone gmRxra-hinge-LBD and gmRxrb2-hinge-LBD (from heart and brain, respectively) into a pSC-B vector through blunt-PCR cloning. This was followed by construction of the two pCMX-GAL4-gmRxra/b2-hinge-LBD expression plasmids through restriction enzyme digestion and ligation. Sanger sequencing was performed to confirm incorporation of the gmRxr into the plasmids and deduced amino acid sequences were aligned in an MSA. Luciferase reporter gene assays were performed to assess ligand activation of the gmRxra/b1/b2/g plasmids in transfected COS-7 cells after ligand exposure. SDS-PAGE and Western blotting were performed to verify Rxr synthesis in COS-7 cells, and cell viability assays were performed to monitor potential cytotoxicity of COS-7 cells after exposure to the test compounds.

3.2 RNA extraction

RNA extraction was performed to clone the subtypes *gmRxra* and *gmRxrb2* from Atlantic cod. The samples used for RNA extraction were heart and brain tissue obtained from a juvenile female Atlantic cod (from the local tissue bank at the environmental toxicology laboratory). Around 30 milligrams of tissue were cut on ice and placed in Eppendorf tubes. 500 µL Trizol was added, and the tissue was homogenized manually with a homogenizer until dissolved. Next, 500 µL (total volume of 1 mL) Trizol was added, and the tube was turned a few times to mix properly, followed by incubation on ice for 5 minutes. 200 µL chloroform was added next, and the tube was shaken for 30 seconds followed by a 5-minute incubation at room temperature. Then, the samples were centrifuged at 12 000 x *g* at 4°C for 15 minutes, which makes the contents separate into two phases (Heraeus multifuge X3R). The upper aqueous phase was transferred into new tubes where 300 µL isopropanol was added. After turning the tube a few times, the tubes were left at room temperature for 5 minutes. Next, the samples were centrifuged again at 12 000 x *g* at 4°C for 10 minutes (Heraeus multifuge X3R). After the centrifugation, all liquid was removed so the only content left was a pellet at the side of the bottom of the tube. Next, 1 mL 75% ethanol was added, and the tubes were vortexed quickly, so the pellet detached from the tube and then centrifuged again at 7500 x *g* at 4°C for 5 minutes. The wash was repeated by removing the supernatant, keeping the pellet in the tube. Then, after removing most of the supernatant without disturbing the pellet, the tubes were left to dry for around 30 minutes at room temperature. During this time, the pellets went from white to transparent and all the ethanol evaporated. Next, 50 µL RNA-free H_2O was added, followed by an incubation at 60°C for 20 minutes. The samples were vortexed once for 5 minutes after the incubation, and then left on ice. The concentrations were measured with Nanodrop 1000 (absorbance ratio $A_{260nm/280nm}$), and the samples were run on a 0.75% agarose electrophoresis gel to check RNA purity and integrity.

The 0.75% agarose gel was prepared by mixing 1.125 gram agarose and 150 mL 1X TAE-buffer which was heated to the agarose dissolved, and then cooled to about 60°C. 50 mL agarose solution was transferred to a 50 mL tube and 0.5 µL GelRed was added and mixed by turning the tube a few times. This mix was then added to the gel casting chamber and a comb to form the gel was inserted. For sample preparation, 5 µL formamide, 1 µL 10X loading buffer and 3.5 µL dH_2O was needed per reaction. 9.5 µL of this mix and 0.5 µL of RNA sample was added to a new tube and mixed with a pipette. The samples were then heated for 10 minutes in a 60°C incubator and were spun down afterwards, and added to the polymerized gel and run at 100V

for approx. 1 hour. Nucleic acids were visualized by gel imaging with ChemiDoc XRS+ (Bio-Rad). The RNA samples were stored at -80°C after running the gel.

3.4 Complementary DNA (cDNA) synthesis

To synthesize complementary DNA (cDNA), the protocol for SuperScript® IV-First-Strand cDNA Synthesis Reaction was used. The first step was to anneal primers to template RNA by combining Oligo $d(T)_{20}$, dNTP mix, template RNA, and nuclease free H_2O as listed in table 34. Oligo $d(T)_{20}$ is a primer consisting of strings of 20 deoxythymidylic acid residues which bind and hybridize to the poly(A) tale of mRNA. The components were briefly centrifuged and then heated at 65°C for 5 minutes. After this, the RNA-primer mix was incubated on ice for at least 1 minute. Next step was to prepare RT reaction mix consisting of 5x SSIV buffer, 100 mM DTT, RNaseOUT™ Recombinant RNase Inhibitor, and SuperScript™ IV Reverse Transcriptase (200 U/µL) (Table 35). 5X SSIV buffer was vortexed and centrifuged before combined with the other components. The reaction mix was mixed by briefly centrifuging. After this, the RT reaction mix was added to the annealed RNA, and the combined mixture was incubated at 53°C for 10 minutes. Then, the reaction mix was incubated at 80°C for 10 minutes to inactivate the reaction. The next step was to remove RNA-degrading enzymes by adding 1 µL *E. coli* RNase H followed by an incubation at 37°C for 20 minutes. The reaction mix was then stored at -20°C and used for PCR amplification the following day using a T100™ Thermal Cycler.

Table 34: RNA-primer mix for anneal step in cDNA for one reaction

Reagents	Volume	Concentration
Oligo $d(T)_{20}$	1µL	50 µM
dNTP mix (10 mM each)	1 µL	10 mM
Template RNA	Up to 11 µL	-
Nuclease free H_2O	To 13 µL	-

Table 35: RT reaction mix for cDNA synthesis

Components	Volume	Concentration
5x SSIV Buffer	4 µL	1X
100 mM DTT	1 µL	100 mM
RNaseOUT^{TM} Recombinant RNase Inhibitor	1 µL	-
SuperScript® IV Reverse Transcriptase	1 µL	200 U/µL

3.5 Polymerase chain reaction

Polymerase chain reaction (PCR) is a method used to produce DNA sequences from a primary pool by using single stranded DNA primers. This process usually begins with preparation of a master mix that contains buffer, primers, dNTPs, polymerase, and template DNA before performing a PCR program. For the PCR protocol of this study, there are three cyclical steps to produce DNA copies: denaturation, annealing and elongation. During denaturation, often occurring at 95°C, the double helix breaks into two separate strands. During annealing, temperatures are adjusted and lowered to which primers can optimally and efficiently bind to 5'-DNA and 3'-DNA. During elongation, the temperature is increased to 72°C which is optimal for DNA-polymerase binding and activation. This synthesizes new strands and allows new double helix formation, which ultimately leads to double amount of DNA helices. This cycle will be repeated typically 20-40 cycles, or until needed amount of DNA (which increases exponentially) is produced.

3.6 Construction of pSC-B-gmRxr plasmid by blunt-end PCR cloning

3.6.1 Primers and PCR amplification of Rxr sequence from cDNA

For amplification of the gmRxr-hinge-LBD DNA sequences from synthesized cDNA, specific primer pairs were used (forward (5') and reverse (3')) together with the other reagents needed for PCR amplification (Table 36). The forward primer and reverse primer were designed to bind at the N-terminal end of the hinge-region and at the C-terminal of the LBD, respectively. The DNA fragments amplified were needed for construction of pSC-B-gmRxr-hinge-LBD and pCMX-GAL4-gmRxr-hinge-LBD plasmids. Restriction enzymes with recognition sites for EcoRI and NheI (forward and reverse) were introduced by the primers listed in table 37 to

construct pCMX-GAL4-gmRxr-hinge-LBD plasmids. The PCR programs used are listed in table 38 and 39.

Table 36: Reagents used for PCR amplification

Components	Volume (µL)	Concentration
MQH_2O	11.4	-
5x Phusion HF buffer	4.0	1X
dNTP	0.4	10 µM
Forward primer	1.0	0.5 µM
Reverse primer	1.0	0.5 µM
cDNA template	2.0	-
DNA polymerase Hot start	0.2	1 U

Table 37: Primers used for PCR amplification

Primers	Type	Sequence
MT2044	gmRxraEcoRI fwd.	GTAGTTGAATTCTTACACGCAGCCGTTCAGGA
MT2046	gmRxra_NHeI rev.	ttgacaGCTAGCCTATGTCATCTGATGTGGTGC
MT2048	gmRxrbEcoRI fwd.	GTAGTTGAATTCGAACGTCAGAGATCGGTGCA
MT2049	gmRxrbNHeI rev.	ttaataGCTAGCCTATGGGAGCTGGTGCGGGG

Table 38: PCR program used for gmRxra

Temperature	Time	Cycles
98	30 seconds	-
98	10 seconds	
63	40 seconds	40
72	30 seconds	
72	5 minutes	
4	∞	-

Table 39: PCR program used for gmRxrb2

Temperature	Time	Cycles
98	30 seconds	-
98	10 seconds	
65	30 seconds	35
72	30 seconds	
72	5 minutes	
4	∞	-

3.7 Agarose gel electrophoresis

Agarose gel electrophoresis was used to analyze amplified DNA. By using this method, it is possible to separate different sizes of DNA strands based on migration through an electric field. The agarose gel is porous, so smaller molecules will migrate longer distances through the gel. DNA has a negative charge, so it will migrate towards a positive electrode.

To perform electrophoresis with an agarose gel, agarose and 1X TAE buffer was mixed to produce 0.70-0.75% agarose and then heated so the components would mix. For one agarose gel, 50 mL of TAE-buffer and 37 milligrams of agarose was needed. After this, 0.5 µL GelRed, a fluorescent nucleic acid dye, was added to the gel solution. This is used to stain and visualize the separated DNA. A comb is used to create wells in the gel. After the gel was set, 1X TAE was poured into the electrophoresis chamber until it covered the gel. At this point, the PCR products were mixed with 10x loading buffer to ensure that the samples would sink to the bottom of the wells. Moreover, a 2-log DNA ladder was used as a reference regarding the size of the PCR products. Lastly, the gel was run at 80V for 1 hour and 15 minutes and then visualized with the instrument ChemiDoc XRS+ (Bio-Rad).

3.8 Gel extraction of DNA

After visualizing the gel, the desired DNA bands were extracted and purified using Zymoclean™ Gel DNA Recovery Kit (ZYMO Research). The gel was placed at a UV-table to visualize the bands with DNA fragments and then cut out by using a scalpel. After this, the bands were moved to Eppendorf tubes, mixed with the calculated volume of ABD (3x volume of sample) and incubated at 50°C for 5-10 minutes or until gel was completely dissolved. Next,

the DNA solution was transferred to a Zymo-Spin column with a column matrix in a collection tube. The tube was centrifuged for 30 seconds, and the flow-through was discarded. All centrifugations were performed at 10 000 x *g*. Next, 200 µL DNA buffer was added, followed by another 30 second centrifugation. After this, at least 6 µL DNA solution buffer must be added (used 12 µL) directly to the column matrix. For the last 30-second centrifugation, it is important to transfer the column into a 1.5 mL Eppendorf tube, as the flow-through contains the eluted DNA. The eluted DNA was measured with Nanodrop 1000 (absorbance ratio $A_{260nm/280nm}$) and stored at -20°C.

3.9 Blunt PCR cloning

Blunt PCR cloning was performed to clone gmRxr-PCR-products into pSC-B vectors by using the StrataClone Blunt PCR cloning kit (Agilent). This created pSC-B-gmRxr-hinge-LBD plasmids. The purified PCR products from the agarose gel were extracted and mixed with StrataClone blunt cloning buffer and StrataClone blunt vector mix. This mix was then incubated for 5 minutes at room temperature before it was placed on ice. The constructed plasmids were transformed into competent *Escherichia coli* (*E. coli*) cells (StrataClone Solopack Competent Cells).

3.9.1 *Escherichia coli* transformation

The StrataClone *E. coli* cells stored at -80°C were first thawed on ice. Then, a ligation mix was made, consisting of 1.5 µl blunt cloning buffer, 1 µl extracted PCR product and 0.5 µl blunt vector mix (Table 40). 1 µl of this ligation mix was added to the cells, followed by incubation on ice for 20 minutes. During the incubation, 3 mL of LB-medium was pre-warmed in a water bath at 42°C. After the incubation, the cells were heat-shocked in a water bath at 42°C for 45 seconds, followed directly by incubation on ice for 2 minutes. Then, 250 µl of pre-warmed LB-medium was added to the cells, followed by centrifugation at 250 rpm for 1 hour and 30 minutes. The tubes were placed horizontally during the incubation period for better aeration. After this, 40 µl 2% X-gal was added to agar-plates. For each receptor, two cell concentrations in two separate agar-plates were used for colony growth. 5 µl of cells was added to one plate together with 50 µl LB-medium making it easier to spread evenly, and 100 µl of the cell mix was added to the other plate. The contents were evenly distributed by using a sterilized glass

rod, and the plates were incubated at 37°C overnight or until transformed *E. coli* colonies were appearing.

Table 40: Reagents used in blunt cloning and PCR product screening

Reagents	Volume
PCR product	1 µL
StrataClone competent *E. coli*	
StrataClone blunt cloning buffer	1.5 µL
StrataClone blunt vector mix	0.5 µL
2% X-gal	40 µL
LB-medium	250 µL / 50 µL

3.9.2 Blue-white colony screening

Blue-white screening was performed to separate transformed and non-transformed bacterial colonies. For this method, 2% X-gal was used as a screening agent. The pSC-B vector used in transformation of the competent *E. coli* cells contained a gene resistant to ampicillin, and therefore only the cells that had taken up the plasmid would grow on the LB-agar plates with ampicillin. The plasmid pSC-B in recombinant cells will disrupt a-complementation which stops b-galactosidase synthesis, as it contains a segment of the lacZ gene. This causes the bacterial colonies to have a white appearance. Cells with non-recombinant plasmid will produce b-galactosidase which metabolizes X-gal resulting in a blue pigment. Therefore, the desired white colonies containing recombinant cells were isolated. Half of the colony will be purified through miniprep, while the other half will be used in a colony PCR.

3.9.3 Colony PCR

Colony PCR was used to confirm the presence of introduced DNA insert in the constructed pSC-B-gmRxr-hinge-LBD plasmid (Table 41, 42 and 43). After PCR amplification, colonies are grown on agar plates until desired size. Preferred colonies were poked using a pipette tip and then mixed into 5 µl MQH_2O in an Eppendorf tube. This mix was then added to a master-mix and amplified with PCR. To confirm the inserted gmRxr-hinge-LBD sequence in the pSC-

B plasmid, agarose gel electrophoresis was used with a 0.7% agarose gel to visualize the PCR products.

Table 41: Reagents used for colony PCR (one reaction)

Reagents	Volumes	Concentrations
10X DreamTaq Green Buffer	1 µL	1X
dNTP	0.8 µL	2.5 µM
Primer (fwd+rev)	0.2 µL	10 µM
Template	0.5 µL	0.5 µM
DreamTaq DNA polymerase	0.05 µL	1X
MQH2O	7.25 µL	-

Table 42: Primers used for colony PCR

Primers	Type	Sequence 5'- 3'
MT2041	pSC-B fwd.	ATTAACCCTCACTAAAGGGA
MT2042	pSC-B rev.	TAATACGACTCACTATAGGG

Table 43: Colony PCR program

Temperature (°C)	Time	Cycles
95	3 minutes	-
95	30 seconds	
45	30 seconds	30
72	1 minute	
72	5 minutes	-
4	∞	-

3.9.4 Plasmid purification

During construction and sequencing of plasmid vectors, both miniprep and midiprep were used to purify plasmid DNA. The two methods have in common that cells are grown in LB-medium and antibiotics (ampicillin in this study), followed by centrifugation and addition of a resuspension buffer. After this, the cells are lysed, and a neutralization buffer is added. This keeps the plasmid DNA supercoiled, while the other cellular components can be precipitated through centrifugation. The supercoiled plasmid DNA will therefore be isolated and stuck to a silica-based membrane in a tube. This is followed by washing, using an ethanol-based buffer. To free purified DNA from the membrane, AE-buffer is used. The two methods differ in that midiprep has an additional cleaning step, where isopropanol is used to precipitate DNA, followed by centrifugation, washing with ethanol, and drying. Lastly, the concentrations of plasmid DNA were measured with Nanodrop 1000 (absorbance ratio $A_{260nm/280nm}$).

The miniprep method was used for purifying the constructed pSC-B-gmRxr-hinge-LBD, and also when sequencing the pCMX-GAL4-Rxr-hinge-LBD plasmids. The NucleoSpin® Plasmid (NoLid) kit was used according to the protocol for plasmid purification. The bacterial colonies containing the plasmid construct were added to 6 mL LB-medium and ampicillin (0.1 mg/mL) in 50 mL Falcon tubes and incubated overnight at 37°C at 250 rpm in a Multitron Standard Shaking incubator (Infors HT). After the incubation, 500 µL of each *E. coli* LB culture sample was added to 500 µL of 50% glycerol. These glycerol stocks were stored at -80°C. The rest of the samples were purified through miniprep. Purified plasmid DNA was eluted in 50 µL AE-buffer and the concentration was measured with Nanodrop 1000 (absorbance ratio $A_{260nm/280nm}$). The plasmid DNA was stored at -20°C.

Construction of pCMX-GAL4-gmRxr

3.9.5 Restriction enzyme digestion

The two restriction enzymes EcoRI and NheI were used to digest both the pCMX-GAL4-DBD plasmid and the pSC-B-Rxra/b2 plasmids constructed in this thesis. This was needed to allow incorporation of the gmRxr-hinge-LBD sequence into pCMX-GAL4-DBD eukaryotic expression vector. The specific recognition sites for the restriction enzymes were already existing in pCMX-GAL4 plasmids and were introduced to gmRxr-hinge-LBD PCR products by the primers previously used in DNA amplification.

Four digestion reactions were set up, one for each of the pSC-B-gmRxr plasmids (a/b2/b2d) and one for the pCMX-GAL4 plasmid (vector). The insert reaction had a total volume of 20 µL, but different volumes of templates were used based on plasmid concentrations after miniprep. The vector digestion also had a total volume of 20 µL, and 0.5 µL template (Table 44). These reactions were incubated at 37°C for 1 hour and 30 minutes. After this, the insert reactions were stored at 4°C, whilst the vector reaction was added 1µL Shrimp Alkaline Phosphatase (SAP) and then incubated at 37°C for 30 minutes. SAP dephosphorylates the plasmid by removing the 5'phosphate group made during the digestion reaction to prevent relegation of linearized pCMX-GAL-4-DBD. This was followed by another incubation at 65°C for 15 minutes, which stopped the dephosphorylation reaction. After this, an agarose gel electrophoresis was used to detect the digested products. gmRxr-hinge-LBD and pCMX-GAL4-DBD bands were excised from the gel using a UV-table and a scalpel. To obtain purified DNA from the gel bands, the ZymoClean^{TM} Gel DNA Recovery kit (ZYMO Research) was used. The concentrations of the DNA samples were measured with Nanodrop 1000 (absorbance ratio $A_{260nm/280nm}$).

Table 44: Reagents used for restriction enzyme double digestion. Based on Nanodrop concentrations, different volumes of a/b2/b2d/Pxr DNA templates were used.

Reagent	Volume	Concentration
EcoRI	1 µL	0.375 U/µL
NheI	1 µL	0.375 U/µL
Template (a/b2/b2d/Pxr)	2 µL / 3.1 µL / 13.2 µL / 0.5 µL	1 µg
10X buffer	2 µL	1X
MQH_2O	Up to 20 µL	-
SAP (vector only)	1 µL	1U

3.9.6 Ligation of gmRxr and pCMX-GAL4

After the restriction enzyme digestion, ligation was done to construct the pCMX-GAL4-RXR-hinge-LBD plasmids. This was performed by using the digested plasmid and gmRxra, gmRxrb2, and gmRxrb2d fragments recovered from the gel. This reaction used T4 DNA-ligase, an enzyme which catalyzes production of phosphodiester bonds between phosphate and hydroxyl groups in DNA. A ligation reaction mix was made containing T4 DNA-ligase, gmRxr,

pCMX-GAL4-digested vector, 10X T4 DNA-ligase buffer, and MQH_2O and then incubated at 4°C for around 15 hours (Table 45). This was followed by an incubation in a heating block at 65°C for 15 minutes, which stops the reaction. Then, the mass of inserted DNA required for the ligation reaction was calculated with Formula 2. The molarity ratio of insert (gmRxr-hinge-LBD) and vector (pCMX-GAL4) was 3:1.

Table 45: Reagents used for the ligation of gmRxr-hinge-LBD and pCMX-GAL4

Reagent	Volume	Concentration
10X T4 DNA ligase buffer	1 µL	1X
T4 DNA ligase enzyme	1 µL	35 U/µL
Vector	-	40 ng
Insert	-	20 ng
MQ H_2O	To 10 µL	-

3.9.7 Transformation of plasmid construct

StrataClone Mix&Go Competent Cells were used to transform the plasmid construct pCMX-GAL4-gmRxr-hinge-LBD into *E. coli* cells. These cells were stored at -80°C, and after they were thawed on ice 2 µL of ligation product was added to 50 µL cells and mixed carefully to minimize cell disturbance. After this, 20 µL cell mix was added to one agar plate, and 5 µL cell mix was added to another plate. 15 µL LB-medium was also added to the last plate with 5 µL cell mix. The cell mixes were evenly distributed by using a sterilized glass rod. This was repeated for all the plasmid constructs. The plates were then incubated for 24 hours at 37°C. The next step was to confirm transformants containing the pCMX-GAL4-Rxr-hinge-LBD plasmids by performing colony PCR and agarose gel electrophoresis. Primers used for colony PCR are indicated in table 46. Lastly, the plasmids were purified through miniprep.

Table 46: Primers used for colony PCR of pCMX

Primers	Type	Sequence 5'-3'
MT1077	pCMX fwd.	TGCCGTCACAGATAGATTGG
MT1279	pCMX rev.	AATCTCTGTAGGTAGTTTGTCCA

3.9.8 Sanger sequencing

Sequencing of pCMX-GAL4-Rxr-hinge-LBD constructs were carried out by the Department of Biological Sciences (UiB), and preparation of the sequencing reaction was done by following the BigDye protocol provided by UiB. This was performed to confirm incorporation of gmRxr-hinge-LBD into pCMX-GAL4 vector. For the reaction, the template pCMX-GAL4-Rxr-hinge-LBD plasmids was mixed with the other reagents on ice and then amplified through PCR (Table 47, 48 and 49). After this, 10 µl MQH_2O was added to all the products and sent for sequencing. The sequencing data was then analyzed in the SnapGene software.

Table 47: Preparation before Sanger sequencing for one reaction

Reagents	**Volume (µL)**	**Concentration**
Fwd. primer	1	3.2 µM
Rev. primer	1	3.2 µM
5X Sequencing buffer	1	1X
Big Dye	1	1U
Template	1	-
MQH2O	To 10 µL	-

Table 48: Primers used for Sanger sequencing

Primers	Type	Sequence 5'-3'
MT1077	pCMX fwd.	TGCCGTCACAGATAGATTGG
MT1279	pCMX rev.	AATCTCTGTAGGTAGTTTGTCCA
MT2281	gmRxr mid.	AGCTGTTCacgCTGGTGGAGTG
MT1383	GAL4 fwd.	ATGAAGCTACTGTCTTCTATCG
MT2066	GAL4 rev.	CGATACAGTCAACTGTCTTTGAC

Table 49: PCR program performed before Sanger sequencing

Temperature (°C)	Time	Cycles
96	5 minutes	-
96 52 60	10 seconds 5 seconds 4 minutes	25
4	-	-

3.9.9 Plasmid purification - midiprep

Midiprep was used to purify the constructed pCMX-GAL4-Rxra/b2/b2d-hinge-LBD plasmids, and the other plasmids needed for luciferase reporter gene assay; gmRxrb1, gmRxrg, b-galactosidase normalization plasmid and luciferase reporter plasmids. The NucleoBond® PC100 kit (Machery-Nagel) was used for midiprep plasmid purification. Cells containing the plasmids were stored in glycerol stocks at -80°C, and a generous amount was added to 200 mL LB-medium containing ampicillin (0.1 mg/mL) in an Erlenmeyer culture flask for cultivation overnight in the Multitron Standard Shaking incubator (Infors HT) at 250 rpm at 37°C for 24 hours, or until desired optical density (OD). Ultrospec 10 Cell Density Meter (Biochrom) was used to measure cell density in suspension at 600 nm, and the optical density volume (ODV) = 200 was calculated. After the desired ODV was reached, plasmid purification was performed with midiprep. This method is similar to miniprep, except plasmid DNA is eluted in 5 mL elution buffer, and therefore an additional cleaning step is needed. In this step, DNA is precipitated using isopropanol, centrifuged, then washed with ethanol, before finally dried. Another difference is that the purified plasmid DNA was dissolved in 150 µL of AE-buffer. Then, the concentrations of plasmid DNA were measured with Nanodrop 1000 (absorbance ratio $A_{260nm/280nm}$), and agarose gel electrophoresis was performed to examine the conformations of the purified plasmids.

3.10 Multiple sequence alignment

Multiple sequence alignments (MSA) were constructed with Clustal Omega (EMBL-EBI) by using gmRxra/b2/b2d-hinge-LBD sequences obtained from Sanger sequencing of the cloned genes. Sequences of gmRxrb1/g-hinge-LBD were obtained previously from Borge (2021). The alignments were visualized with JalView 2.11.2.2.

3.11 Western blot assay

3.11.1 Sodium-dodecyl-sulfate (SDS)-polyacrylamide gel electrophoresis (PAGE)

SDS-PAGE is a method used to separate proteins by molecular size. The first step was to mix the proteins with SDS and a sample buffer containing b-mercaptoethanol. This mixture was then heated at 95°C to denaturate the proteins. SDS promotes protein denaturation and coats the polypeptides, producing a negatively charged polypeptide chain that allows migration

through the polyacrylamide gel used for separation of the differently sized proteins. B-mercaptoethanol acts as a reducing agent by breaking disulfide bonds.

3.11.2 Preparation of cell lysates

To prepare cell lysates for the western blot assay, COS-7 cells were seeded and incubated for 24 hours in 96-well plates. The next day, DMEM was changed, and cells were transfected with the different pCMX-GAL4-Rxr plasmids. 24 hours later medium was discarded, and cells were washed with 100 µL PBS. Then, 20 µL lysis reagent was added to each well and cells were incubated on a shaker for 5 minutes on ice. Lastly, lysates were removed from the wells and stored at -80°C.

3.11.3 Protein staining

To separate and visualize protein content, a polyacrylamide gel (1 millimeter) was casted. The gel consisted of a stacking and running gel that was added to an electrophoresis chamber. The chamber was filled up with 1X TGS buffer and the wells were loaded with 5 µL Precision Plus Protein™ Prestained Protein Standards as a molecular weight marker, and 20 µL of each cell lysate (approx. X microgram). The run time for the gel was 80V for 10 minutes, then 150V for 50 minutes. After the run ended, the gel was placed in a small plastic box and stained with InstantBlue™ Coomassie Protein Stain (Expedeon) overnight on a shaker at room temperature. Next day, excess Coomassie was poured off, the gel was destained with ddH_2O. ChemiDoc WRS+ (Bio-Rad) was used for imaging the gel.

3.11.4 Western blotting

Western blotting is a method used to detect specific proteins separated by SDS-PAGE by using antibodies. This was performed to confirm the synthesis of GAL4-Rxr-hinge-LBD fusion protein in transfected COS-7 cells. There are several components needed to create the western blot “sandwich”. The assembly in a specific holder is in the following order: sponge, paper, nitrocellulose membrane, gel, paper, sponge. All components must be submerged in transfer buffer before assembling. The sandwich in the holder was then placed in an electrophoresis chamber filled with transfer buffer and a cooling unit and run for 1 hour at 100V. Next, the membrane was removed from the sandwich and placed into a small box and blocked with TBST

containing 7% dry-milk. Lastly, the membrane was placed on a shaker overnight at 4°C. Next day, the TBST and dry-milk solution was poured off and the membrane was washed 3 times with TBST while shaking for 10 minutes at room temperature. After this, primary monoclonal antibody anti-GAL4-DBD mouse (Santa Cruz) was diluted 1:2000 in TBST and added to the membrane on a shaker overnight at room temperature. The membrane was then rinsed again with TBST three times with 10 minutes shaking in between. Then, secondary antibody horseradish peroxidase-linked antibody sheep anti-mouse IgG (polyclonal) (GE Healthcare) was diluted 1:2000 in TBST, added to the membrane and placed on shaker for 1 hour at room temperature. After this, the membrane was washed again with TBST. Then, a 2 mL solution of SuperSignal™ West Pico PLUS Chemiluminescent Substrate was prepared and poured onto the membrane to visualize the GAL4-Rxr-hinge-LBD proteins. After a 5 minutes incubation at room temperature, ChemiDoc XRS+ (Bio-Rad) was used for imaging of the protein bands.

b-actin was used as a loading control on the same membrane. After washing with TBST, anti-b-actin monoclonal antibody (Abcam) diluted 1:10 000 in TBST was poured onto the membrane and incubated for 1 hour on a shaker at room temperature. After this, the antibody and TBST mix was poured off and the membrane was washed with TBST on a shaker three times for 10 minutes. The secondary Horseradish peroxidase-linked antibody sheep anti-mouse IgG (polyclonal) (GE Healthcare) diluted 1:2000 in TBST was added to the membrane, followed by a 1-hour incubation on a shaker at room temperature. The membrane was washed with TBST and visualized in the same way as with the first blot.

3.12 Luciferase reporter gene assay

Luciferase reporter gene assays were performed to detect and measure ligand-induced activation of the gmRxr subtypes. In each assay, COS-7 cells were transfected with three plasmids, including a b-galactosidase-encoding normalization plasmid, a reporter plasmid (MH100)x4tkluc containing the luciferase reporter gene, and lastly the pCMX-GAL4-Rxr-hinge-LBD receptor plasmid. The b-galactosidase encoding plasmid expresses the b-galactosidase enzyme constitutively and is used to normalize transfection efficiency and COS-7 cell numbers between the different wells (96 well plate). b-galactosidase produces ONP and galactose through hydrolysis of the substrate ONPG, and since ONP absorbs light at 420 nm, the ONP levels can be correlated to b-galactosidase activity. Upstream GAL4-activation sequences (GAL4-UAS) in the promoter region of the reporter-plasmid regulates the

transcription of the luciferase gene. Through ligand binding, the translated receptor will undergo confirmational changes which allows GAL4-Rxr-hinge-LBD binding to the upstream activation sequence (UAS) in the reporter plasmid, promoting transcription and synthesis of the luciferase enzyme. This allows measurement of luciferase enzymatic activity. Luciferin added to lysated cells is converted to oxyluciferin by luciferase, a reaction that simultaneously emits light (550-570 nm). The amount of light emitted is quantified in a luminometer and correlated to levels of gmRxr activation. An overview of the GAL4-UAS based luciferase reporter gene assay is found in figure 8.

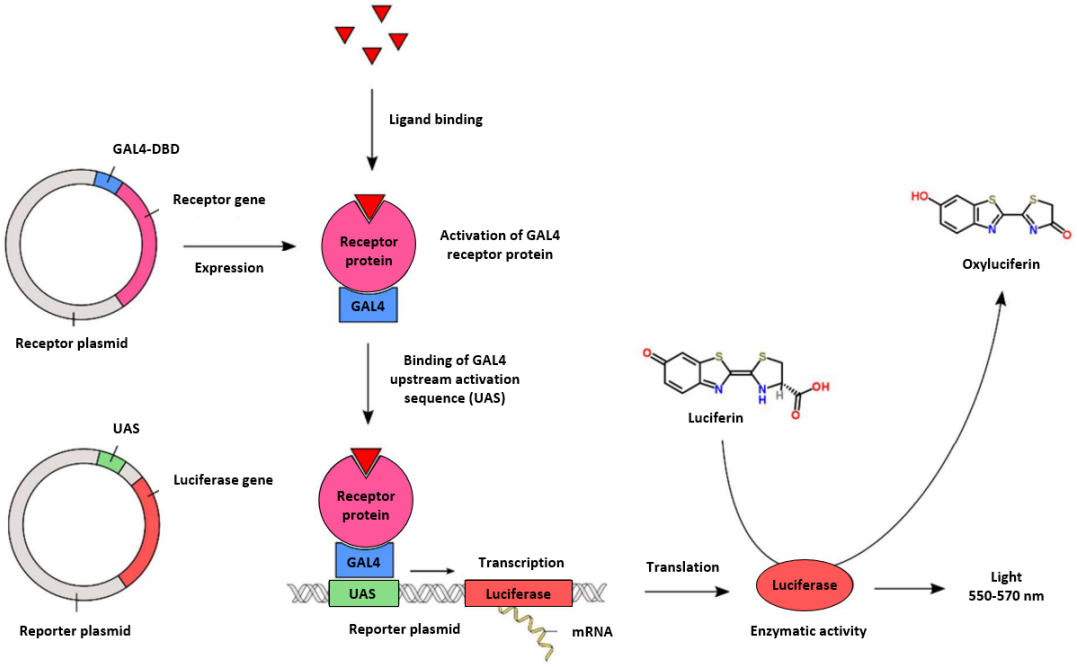

Figure 8: Overview of the GAL4-UAS based luciferase reporter gene assay. Reporter plasmids (luciferase) and receptor plasmids are transfected into a cell line. The GAL4 receptor protein bound to GAL4-DBD becomes activated through ligand binding. Then, GAL4-DBD binds to UAS in the reporter plasmid. Luciferase is subsequently synthesized and catalyzes the transformation of luciferin to oxyluciferin and light. The figure is adapted from Madsen (2016).

3.12.1 Cultivation of COS-7 cells

COS-7 cells were stored in tubes with freezing medium in a liquid nitrogen tank. One of the cell-containing tubes was quickly thawed and added to a 15 mL falcon tube with 10 mL growth medium (DMEM-10%FBS) and centrifuged for 5 minutes at 500 rpm at room temperature in the Heraeus multifuge X3R (Thermo Scientific). Then, the medium was removed, and the pellet was resuspended in new growth medium. Next, the cells were seeded in petri dishes at several

dilutions and incubated at 37°C with 5% CO_2. When the cells reached confluency of 70-90%, the medium was removed, and the cells were washed with 1X PBS two times. After this, 1.5 mL of Trypsine-EDTA (0.05% trypsin and 0.02% EDTA) was added and incubated for 45 seconds before removing. This allows the cells to detach from the bottom of the petri dish. This was followed by a 5-minute incubation at 37°C with 5% CO_2, and then resuspension of the cells with 10 mL growth medium. The cells were diluted 1:20, meaning the new petri dishes contained 9.5 mL growth medium and 0.5 mL cell suspension. After shaking for distributing the cells, the petri dish was placed in an incubator at 37°C with 5% CO_2.

3.12.2 Seeding of COS-7 cells

COS-7 cells were seeded for the first day of luciferase gene reporter assay. COS-7 cells with 70-90% confluency in petri dishes were treated as described above (washed, trypsinated and resuspended), except the suspension was added to a 50 mL Falcon tube. New petri dishes were also prepared for future assays. After this, 50 µL of the cell suspension was added to an Eppendorf tube with 50 µL erythrosine-B which stains the cells for counting in light microscopy. A hemocytometer was used to count cells and calculate cell density, and cells were seeded at a cell density of 5000 cells per well in 96-well plates, with the total volume of growth medium and cell suspension to 100 µL. This was followed by incubation at 37°C with 5% CO_2 for 18-24 hours.

3.12.3 Transfection of COS-7 cells

The following day after seeding, COS-7 cells were transfected with a mixture of (MH100)x4 tk luc, pCMV b-Gal and pCMX-GAL4-Rxr-hinge-LBD (Rxra/b1/b2/b2d/g) (Table 50). Plasmid mix, TransIT-LT1 and Opti-MEM I were mixed and incubated at room temperature for 30 minutes before it was added to fresh DMEM-10% FBS (Table 51). Next, old medium was removed from the 96-well plates and 101 µL of DMEM-transfection mix was added to each well. Lastly, the 96-well plates were incubated at 37°C with 5% CO_2 for 24 hours.

Table 50: Amount plasmid per well

Plasmid	Amount (ng)
(MH100)x4 tk luc	47.62
pCMV-b-Gal	47.62
pCMX-GAL4-Rxra/b1/b2/b2d/g	4.76

Table 51: COS-7 transfection reagents

Reagent	Volume per well (µL)
Opti-MEM I	9.0
Plasmid mix	0.1
TransIT-LT1	0.2
DMEM-10% FBS	92.0

3.12.4 Ligand exposure of COS-7 cells

24 hours after transfection, the COS-7 cells were exposed to ligands. A deep 96-well plate was used to dilute the concentration of the ligands, whereas well A had the highest concentration and declining to well G with the lowest concentrations (Table 52). The ligands were dissolved in DMSO and phenol-red free growth medium (DMEM-10% FBS w/o phenol red), and the dilution factor was 2 from A to B, and 7 for the remaining rows. Well H contained only DMSO and growth medium, and therefore used as a solvent control. The dilution series was made in a 2 X concentration. After this, old medium from the 96-well plates were discarded and 100 µL 2 X dilution mix was added to corresponding wells. Moreover, 100 µL phenol-red free growth medium was added to all wells and mixed gently. This made the 2 X dilution mix into a 1 X concentration of the ligand and the final DMSO concentration to 0.2-0.5%. After this, cells were incubated and exposed at 37°C with 5% CO_2 for 24 hours.

Table 52: Dilutions (µM) used for ligand exposure in luciferase gene reporter assay. Wells in row H only contained a mixture of DMSO and DMEM.

Well	9-cis retinoic acid	Tributyltin chloride	Tripropyltin chloride	Fentin chloride	Fentin hydroxide	Trimethyltin chloride
A	10.0000	0.25000	0.25000	0.25000	0.25000	0.25000
B	5.0000	0.12500	0.12500	0.12500	0.12500	0.12500
C	1.42857	0.03571	0.03571	0.03571	0.03571	0.03571
D	0.20408	0.00510	0.00510	0.00510	0.00510	0.00510
E	0.02915	0.00073	0.00073	0.00073	0.00073	0.00073
F	0.00416	0.00010	0.00010	0.00010	0.00010	0.00010
G	0.00059	0.00001	0.00001	0.00001	0.00001	0.00001
H	-	-	-	-	-	-

3.12.5 Reading – lysis and enzymatic measurements

After 24 hours of exposure, the first step after preparing the three solutions (lysis buffer, b-galactosidase reaction solution and luciferase reaction solution) was to discard the medium in the wells of the 96-well plate, and to add 125 µL lysis buffer. This was followed by a 30-minute incubation period on a shaker (HS 501 Digital) at room temperature, which allows release of b-galactosidase and luciferase in an active state due to the buffers ability to inhibit protease activity and disrupt membrane integrity. After the incubation period, 50 µL of the lysate was transferred to a white luminescence 96-well plate for luciferase activity, and 50 µL was transferred to a transparent 96-well plate for measurement of b-galactosidase activity. Then, 100 µL of luciferase reaction solution was added to the white 96-well plates and immediately read in the Enspire 2300 plate reader (PerkinElmer) for detecting luminescence. 100 µL of b-galactosidase reaction solution was then added to the transparent 96-well plates and incubated for around 20 minutes or until the formation of a yellow color. To adjust variability in transfection efficiency in the results, the luciferase activity was divided by the b-galactosidase activity. The results were presented as non-linear regression curves by using GraphPad Prism 9.

3.13 Cell viability assay

Cell viability assay was performed to monitor potential cytotoxic effects of the ligands on the COS-7 cells used in luciferase reporter gene assays. The resazurin and CFDA-AM assays were used to detect changes in metabolic activity and cell-membrane integrity, respectively. Cells were seeded in 96-well plates and incubated for 48 hours at 37°C and 5% CO_2, leaving some wells empty to record background signals. After the 48-hour incubation, transfected COS-7 cells were exposed to identical concentrations of ligand from the luciferase reporter gene assay and incubated for 24 hours at 37°C and 5% CO_2. Triton X-100 (1%, 0.5%, 0.25%) was used as a positive control for reduced cell viability. After this, medium was removed, and cells were washed with 1XPBS. Then, 100 µL of a resazurin/CFDA-AM mixture was added to each well. The cells were then incubated for 1 hour at 37°C in 5% CO_2. The Enspire 2300 plate reader (PerkinElmer) was used to measure fluorescence signals. Resazurin was measured at 530 nm excitation and 590 nm emission, and CFDA-AM was measured at 485 nm excitation and 530 nm emission. For viewing and visualizing the changes in metabolic activity and membrane integrity, GraphPad Prism 9 was used to plot the data.

4. Results

4.1 Cloning of gmrxra and gmrxrb2 and construction of eukaryotic expression plasmids

4.1.1 RNA extraction and cDNA synthesis

Tissue samples used for RNA extraction (method 3.2) and gene cloning were retrieved from the local tissue bank at the environmental toxicology laboratory. Previous knowledge on the tissue-specific expression of the gmRxr isoforms in Atlantic cod was used when deciding on the tissue types for RNA extraction (Borge, 2021). gmRxra was earlier shown with RT-qPCR to be the least prominent subtype in most tissues, but heart tissue was chosen as it had demonstrated the highest expression this subtype. gmRxrb2 was extracted from brain tissue, as this subtype was most prominent in this tissue. The absorbance ratio $A_{260nm/280nm}$ for the two RNA samples were above 1.8, indicating that the isolated RNA contained low or no contamination of DNA. The $A_{260nm/230nm}$-ratios, which is an indication of solvent impurities, had some variations where the RNA extracted from heart tissue was close to 2 (i.e. low impurity), whereas the $A_{260nm/230nm}$ ratio for RNA extracted from brain tissue was somewhat lower. The integrity of the extracted RNA was assessed with agarose gel electrophoresis (Figure 9). The gel revealed that the extracted RNA samples contained two distinct bands at 1200 and 2300 bp, representing 18S and 28S ribosomal RNA, respectively, indicating sufficient integrity of the RNA for cDNA synthesis.

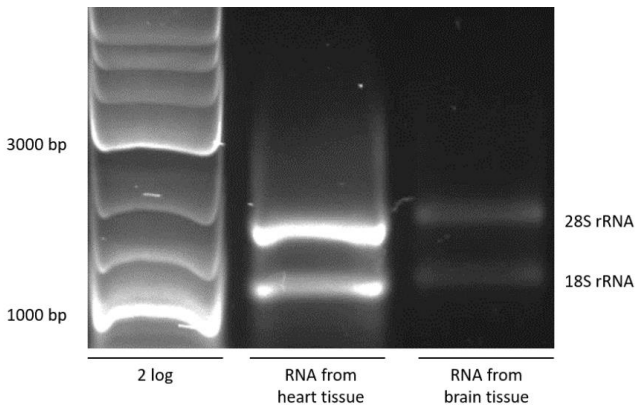

Figure 9: RNA extraction from Atlantic cod heart and brain tissue. The extracted RNA was visualized with agarose gel electrophoresis in a 0.75% agarose gel. 2 log molecular weight standard was included for size estimation of the extracted RNA. Bands representing 28S rRNA and 18S rRNA are indicated.

4.1.2 PCR amplification of gmRxra-hinge-LBD and gmRxrb2-hinge-LBD

PCR was used to amplify the hinge-LBD-encoding parts of the Atlantic cod *gmrxra* and *gmrxrb2* genes from the cDNA prepared from heart and brain tissue, respectively. The PCR reactions were made in three independent reactions for each subtype and using the primers shown in Table 37. These primers were designed to introduce the restriction sites for the enzymes EcoRI and NheI in the amplicons. The amplified PCR products were assessed on a 0.75% agarose gel, which showed bands that migrated according to the expected sizes of the gmRxra-hinge-LBD (813 bp) and gmRxrb2-hinge-LBD (849 bp) DNA fragments (Figure 10). One of the PCR reactions for gmRxrb2 did not produce an amplicon.

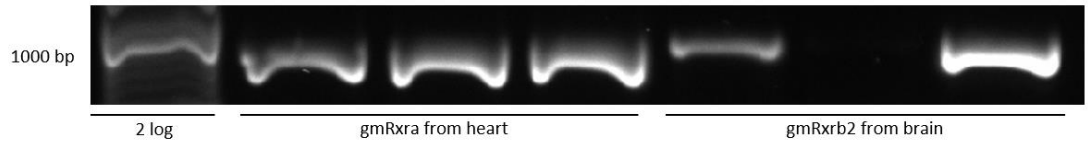

Figure 10: Amplified PCR products from heart and brain cDNA. The PCR products were separated with agarose gel electrophoresis in a 0.75% agarose gel. DNA fragments were visualized with GelRed. The annotations of the PCR products are indicated below the gel. 2 log molecular weight standard was included for size estimation of the PCR products.

4.1.3 Blunt-end PCR cloning and construction of pSC-B-gmRxra/b2-hinge-LBD plasmids

By using blunt-end cloning, the amplified PCR products of gmRxra/b2-hinge-LBD were ligated into the cloning plasmid (pSC-B), creating the pSC-B-gmRxra-hinge-LBD and the pSC-B-gmRxrb2-hinge-LBD plasmids (method 3.6). These plasmids were then transformed into competent *E. coli* cells, followed by cultivation on LB-agar-ampicillin plates for blue-white screening with X-gal. Four white colonies per Rxr subtype were picked from three different plates (total of 12 colonies). Colony PCR (method 3.9.1) and agarose gel electrophoresis were performed to confirm and select positive transformants containing the pSC-B-gmRxra/b2-hinge-LBD plasmids. Since the primers used for the colony PCR bind to the pSC-B vector on each side of the gmRxra/b2-hinge-LBD insert, bands slightly larger than the cloned gmRxra/b2-hinge-LBD fragments were expected. Figure 11 shows incorporation of a fragment of around

1100 bp in size in most clones. Two colonies of positive transformants per plate were used for plasmid purification (miniprep), which made a total of six colonies of pSC-B-gmRxra-hinge-LBD and four colonies of pSC-B-gmRxrb2-hinge-LBD.

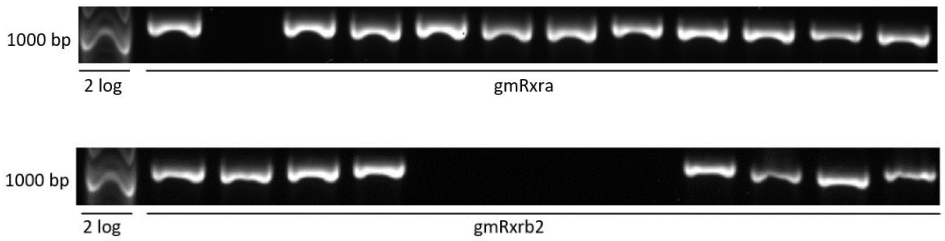

Figure 11: Colony PCR screening to confirm positive pSC-B-Rxra/b2-hinge-LBD transformants after blunt-end cloning. 24 colonies in total were picked from blue-white screening and amplified using PCR. The primers used for the PCR were MT2041 and MT2042. The PCR products were separated and visualized on a 0.75% agarose gel. 2 log molecular weight standard was included for size estimation of PCR products.

4.1.4 Sequencing pSC-B-Rxra/b2-hinge-LBD plasmids

The pSC-B-gmRxra-hinge-LBD and pSC-B-gmRxrb2-hinge-LBD plasmids were isolated through miniprep, and Sanger sequencing was performed to sequence the inserted DNA in the pSC-B-Rxra/b2 plasmids and confirm cloning of the correct DNA fragments (method 3.9.8). When sequencing the expected variants of Rxra and Rxrb2, the resulting sequences revealed that several of the Rxrb2-clones consistently lacked an internal stretch of 42 nucleotides (corresponding to 14 aa-residues). This was considered as a Rxrb2 splice variant and was therefore decided to be included in the following analyses. The splice variant was named gmRxrb2d.

4.1.5 Construction of the pCMX-GAL4-Rxra/b2/b2d-hinge LBD expression plasmids

Double digestion reactions were performed to construct the three pCMX-GAL4-Rxra/b2/b2d-hinge-LBD expression plasmids (method 3.9.5). By using the restriction enzymes EcoRI (3’ end) and NheI (5’end), the gmRxra/b2/b2d-hinge-LBD fragments could be excised from pSC-B-gmRxra/b2/b2d-hinge-LBD plasmids. This is due to the restriction enzyme recognition sites that were introduced with the primers used during the blunt-end cloning. The previously constructed pCMX-GAL4-Pxr plasmid from hake (*Merluccius merluccius*) was simultaneously digested with the same restriction enzymes to produce an empty vector. This plasmid already

contained the recognition sites for EcoRI and NheI. Therefore, the restriction enzymes were used to digest both pSC-B-gmRxra/b2/b2d-hinge-LBD and pCMX-GAL4-Pxr plasmids, giving compatible ends needed for ligation. SAP was added to the digested pCMX-GAL4 vector to inhibit relegation of linearized DNA.

The digested plasmids were separated on a 0.7% agarose gel as shown in figure 12. For the gmRxr-containing plasmids, the slowest migrating bands indicate both undigested pSC-B-Rxra/b2/b2d-hinge-LBD and empty pSC-B (~3000 bp), whilst the fastest migrating bands represent the three gmRxra/b2/b2d-hinge-LBD digested fragments. For the pCMX-GAL4-Pxr plasmid, the slowest migrating band indicates the digested pCMX-GAL4-DBD vector fragment, whilst the fastest migrating band represents the digested hake Pxr fragment. The fragments representing gmRxra/b2/b2d-hinge-LBD and the pCMX-GAL4-DBD empty vector (indicated by blue boxes in figure 12) were excised from the agarose gel and purified as described in method 3.9.5.

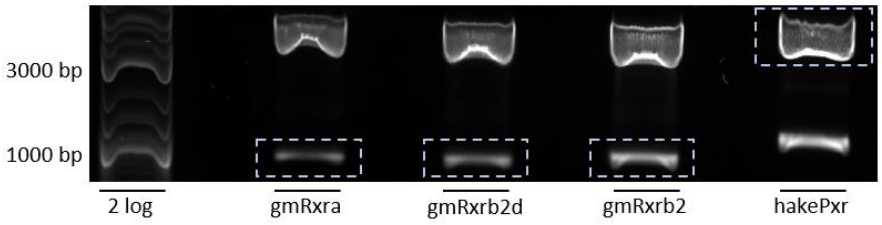

Figure 12: Restriction enzyme digestion of pSC-B-Rxra/b2/b2d-hinge-LBD plasmids and pCMX-GAL4-Pxr plasmid. Digestion-products were analyzed with 0.7% agarose gel electrophoresis. The slowest migrating bands above 3000 bp represent the undigested/empty pSC-B-Rxra/b2/b2d-hinge-LBD and undigested/empty pSC-B (the size difference is too small to differentiate the two DNA fragments). The gmRxra/b2/b2d-hinge-LBD and pCMX-GAL4-DBD fragments indicated in blue boxes were excised from the gel and purified. 2 log molecular weight standard was used as molecular weight marker.

The extracted and purified gmRxra/b2/b2d-hinge-LBD and empty pCMX-GAL4-LBD fragments were then mixed and ligated, so the ligation products could be used to transform competent *E. coli* cells (method 3.9.6). These cells were then cultivated and grown on LB-agar-ampicillin plates and colony PCR was performed to confirm transformation and ligation of the three pCMX-GAL4-gmRxr-hinge-LBD plasmids. Eight colonies of transformants were assessed and using primer flanking the inserts (total of 24 colonies). The resulting amplicons were visualized on a 0.7% agarose gel (Figure 13). Three colonies from each subtype (gmRxra,

gmRxrb2, gmRxrb2d) were chosen for purification of plasmids with miniprep, which were subsequently sequenced with Sanger sequencing to ensure correct insertion of the -Rxra/b2/b2d fragments into the pCMX-GAL4 vector (3.9.8). The sequencing confirmed incorporation of the gmRxra/b2/b2d into the pCMX-GAL4-DBD plasmid in correct reading frame and fused to the GAL4-DBD domain, creating pCMX-GAL4-gmRxra-hinge-LBD, pCMX-GAL4-gmRxrb2-hinge-LBD and pCMX-GAL4-gmRxrb2d-hinge-LBD.

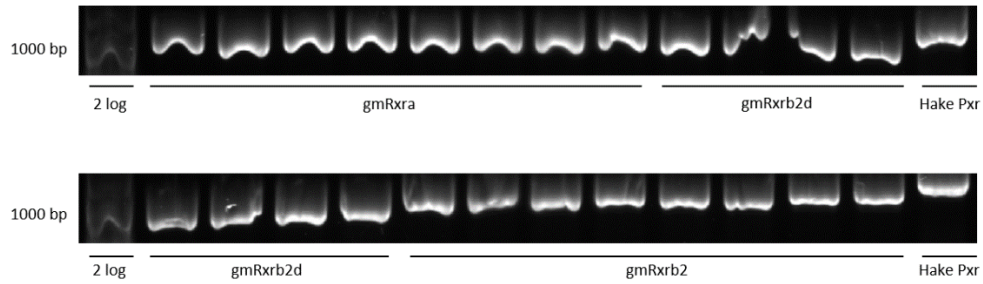

Figure 13: Colony screening of pCMX-GAL4-gmRxra/b2/b2d-hinge-LBD transformants. The transformants were visualized with agarose gel electrophoresis on a 0.7% agarose gel. Three colonies from each subtype were chosen for miniprep. 2-log DNA ladder was used as a molecular weight marker.

Midiprep was used to purify the constructed pCMX-GAL4-Rxra/b2/b2d-hinge-LBD plasmids, as well as the gmRxrb1, gmRxrg, b-galactosidase normalization plasmid and luciferase reporter plasmids needed for the luciferase reporter gene assay (method 3.9.9). After inoculation, the plasmids were purified through midiprep. The purified plasmids were then assessed with agarose gel electrophoresis on a 0.7% agarose gel to examine plasmid conformations (Figure 14). The plasmids demonstrated a supercoiled conformation, promoting an efficient transfection into COS-7 cells.

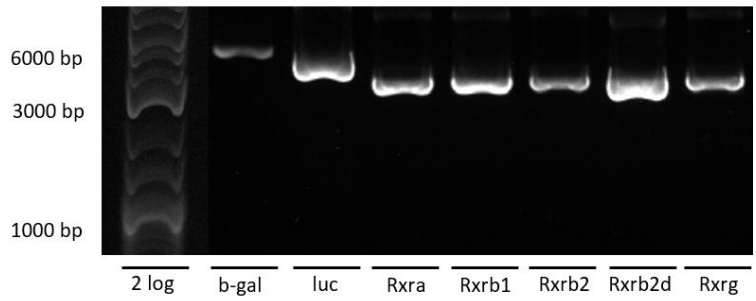

Figure 14: Agarose gel electrophoresis of plasmids used for the luciferase reporter gene assay. The plasmid samples were separated on a 0.75% agarose gel to examine structural conformation. The abbreviations indicate: b-gal – pCMV-b-gal, luc - (MH100)x4 tk luc. A 2-log DNA ladder was used as a molecular weight marker.

4.2 Confirmation of GAL4-Rxra/b2-hinge-LBD fusion protein synthesis in transfected COS-7 cells

Before the luciferase reporter gene analyses were conducted with the Rxr hinge-LBD subtypes, their synthesis in COS-7 cells after transfection was assessed with Western blotting (method 3.11). COS-7 cells were seeded for 48 hours and then transfected with the GAL4-DBD-Rxra/b1/b2/b2d/g-hinge-LBD plasmids for 24 hours. Cell lysates were separated with SDS-PAGE where one parallel gel was stained with Coomassie Brilliant Blue to confirm the electrophoretic separation of the polypeptides. The staining revealed adequate protein separation and about the same amount of protein content distributed in each well (Figure 15).

Western blotting was performed using the second gel to detect synthesis of GAL4-Rxra/b1/b2/b2d/g-hinge-LBD fusion proteins, while anti b-actin antibody was used as a positive loading control. The fusion proteins GAL-Rxra/b1/b2d/b2/g-hinge-LBD formed immunoreactive bands at 46-48 kDa, which was the approx. expected migration according to predicted molecular weights. As expected, only the transfected cells produced GAL4 immunoreactive bands, whereas b-actin was detected in both transfected and non-transfected cells. This confirms the expression and synthesis of the desired fusion proteins in the transfected COS-7 cells (Figure 15).

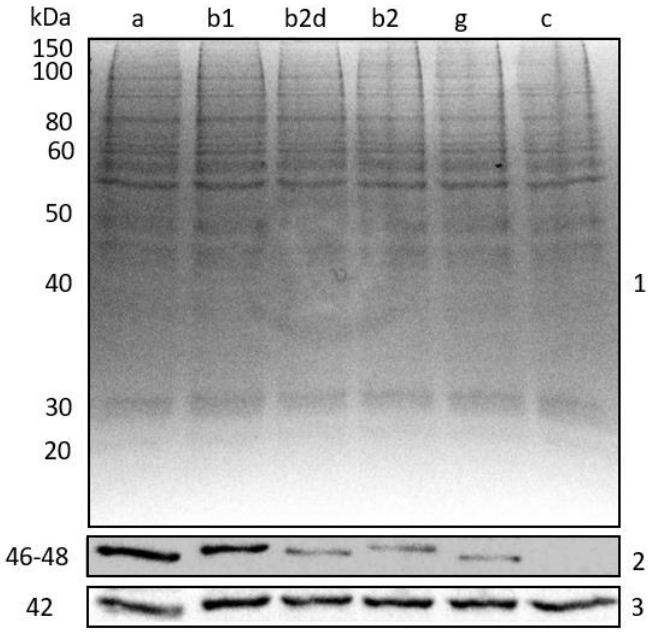

Figure 15: Detection of GAL4-Rxra/b1/b2/b2d/g-hinge-LBD fusion proteins in transfected COS7-cells with Western blotting. The cell lysates from COS-7 cells transfected with either gmRxra, gmRxrb1, gmRxrb2d, gmRxrb2 or gmRxrg are indicated above the gel in panel 1. The abbreviations indicate: a – gmRxra, b1 – gmRxrb1, b2d – gmRxrb2d, b2 – gmRxrb2, g – gmRxrg, and c – non-transfected cells. (1) Total protein staining of SDS-PAGE gel with Coomassie Brilliant Blue. (2) Nitrocellulose membrane first treated with the primary antibody mouse anti-GAL4, and then treated with a secondary antibody sheep anti-mouse-IgG. (3) The same nitrocellulose membrane as shown in (2) but treated with mouse anti-b-actin antibodies and sheep anti-mouse-IgG to reveal b-actin. The immunoreactive bands were visualized by using SuperSignal^{TM} West Pico PLUS Chemiluminescent Substrate.

4.3 Luciferase reporter gene assay

After COS-7 cells were seeded, they were transfected with a plasmid mix containing (mh100)x4tk luc (reporter plasmid) and pCMV-b-gal (normalization plasmid), in addition to constructed pCMX-Rxr-hinge-LBD containing either the Rxra, Rxrb1, Rxrb2, Rxrb2d, or Rxrg. Transfection was followed by a 24-hour exposure to diluted concentrations of 9-cis RA and the following organotins: TBT, TPT, FH, FC and TMTC. This was followed by measuring the enzymatic activity of luciferase and b-galactosidase in COS-7 lysates through luminescence and absorbance readings, respectively. The fold change in gmRxra/b1/b2/b2d/g activation was calculated from normalized luciferase activity and compared to a DMSO solvent control. b-galactosidase activities were used for normalization of transfection efficiencies. Average fold activation was calculated through triplicate measurements in three separate assays.

4.3.1 Ligand activation of gmRxra/b1/b2/b2g/g-hinge-LBD

The ligand activation of gmRxra/b1/b2/b2d/g-hinge-LBD was assessed with luciferase gene reporter assays (method 3.12) and visualized as dose-response curves with GraphPad Prism 9 (Figure 16). 9-cis RA induced activation of gmRxra, gmRxrb2d and gmRxrg, while no significant activation was observed in gmRxrb1 and gmRxrb2 after 9-cis RA exposure (Appendix Table A). The highest maximum fold activation was observed for gmRxra, with E_{max} of 292-fold activation at 5 µM, and the lowest observed maximum fold activation among the activated subtypes was observed for gmRxrg, with an E_{max} of 72-fold activation at 10 µM (Table 53). EC_{50} values for gmRxra, gmRxrb2d were not calculated as a plateau of activation was not reached. The EC_{50} for gmRxrg was 0.06 µM.

Similar to the results obtained for 9-cis RA, all organotins except TMTC produced significant activation of gmRxra, gmRxrb2d and gmRxrg (Figure 16 and Appendix Table B). TBT appeared to produce a higher efficacy than the other organotins across all receptors, as gmRxra, gmRxrb2d and gmRxrg produced the highest levels of fold activation when exposed to this ligand. The observed maximum fold activation for gmRxra after TBT exposure was 510 at 0.25 µM, while gmRxrb2d and gmRxrg produced an E_{max} of 177 at 0.25 µM and 70 at 0.25 µM, respectively (Table 53). TPT exposure caused an E_{max} of 350.5 for gmRxra, 118.5 for gmRxrb2d and 47.2 for gmRxrg. FH and FC induced similar activation levels but at lower concentrations than TBT and TPT. For instance, gmRxra had fold change induction levels at 160 when exposed to 0.005 µM TBT, whereas the E_{max} for FH was 200 at 0.125 µM and E_{max} for FC exposure was 93 at 0.25 µM.

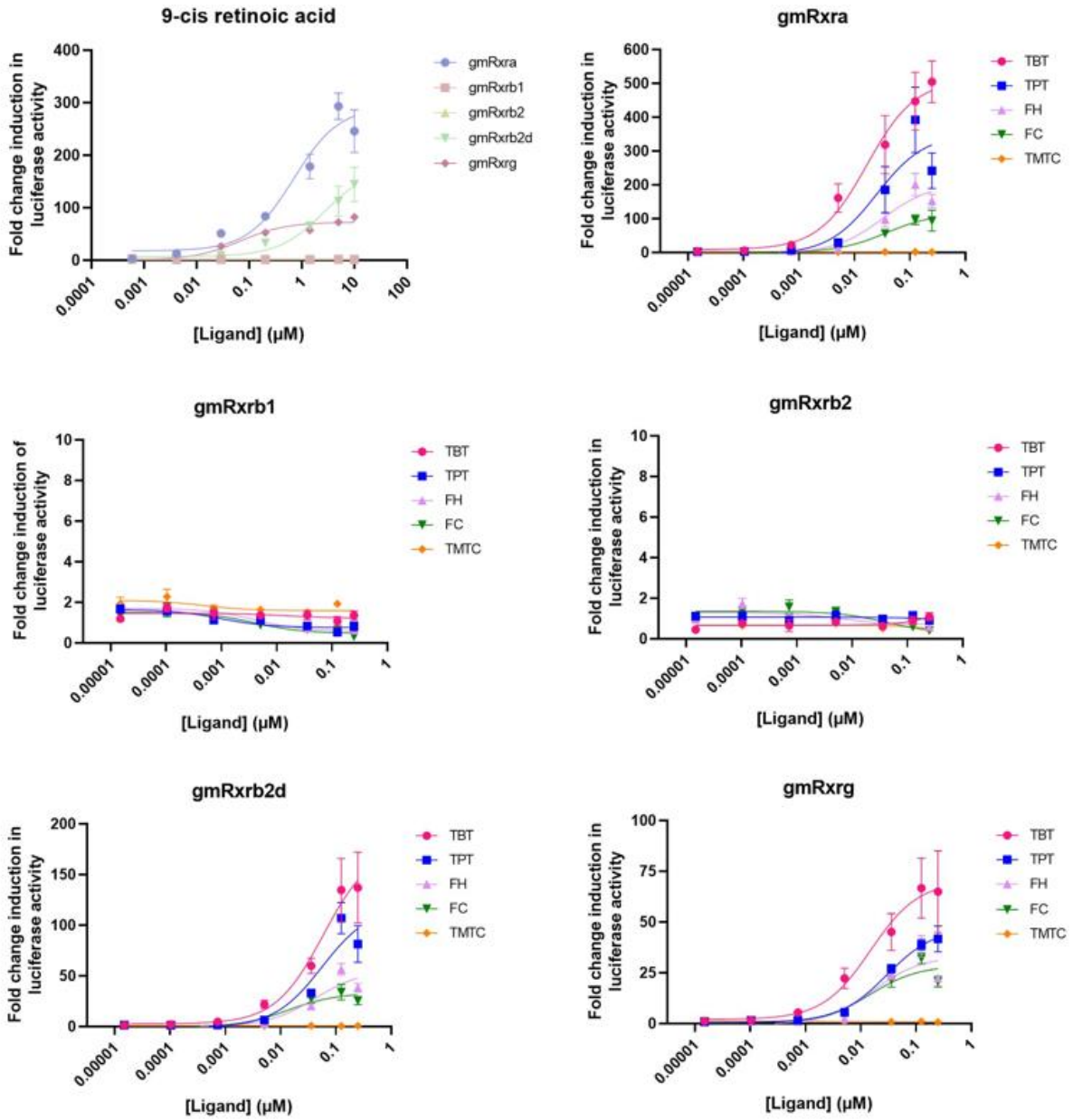

Figure 16: Ligand activation of gmRxra, gmRxrb1, gmRxrb2, gmRxrb2d and gmRxrg by TBT, TPT, FH, FC, TMTC and 9-cis RA. Each point in the dose-response curves represents gmRxra/b1/b2/b2d/g with relative fold change in luciferase activity compared to DMSO-exposed cells. The points are average activation of triplicate concentrations obtained from three separate experiments. Standard error of mean (SEM) is shown. The dose-response curves were produced in GraphPad Prism 9.

Table 53: LOEC, EC_{50} and E_{max} for gmRxra/b2/g activated by 9-cis RA and the organotins TBT, TPT, FC and FH. LOEC (µM), EC_{50} (µM) and maximum fold activation were calculated in GraphPad Prism 9, and the statistical significance of E_{max} (p-value) was calculated with Kruskal-Wallis test with Dunn's multiple comparisons test.

Receptor	Agonist	Lowest observed effect concentration (LOEC) (µM)	Half maximal effective concentration 50 (EC_{50}) (µM)	Maximum fold activation (E_{max})	p-value (E_{max})
gmRxra	9-cis RA	0.0291	0.702	292.3	<0.0001
	TBT	0.0051	0.016	510.3	<0.0001
	TPT	0.0051	0.025	350.5	<0.0001
	FC	0.0051	0.037	115.7	<0.0001
	FH	0.0051	0.032	204.3	<0.0001
	TMTC	-	-	-	-
gmRxrb2d	9-cis RA	0.2040	*	176.0	<0.0001
	TBT	0.0051	0.058	177.6	<0.0001
	TPT	0.0051	0.056	118.5	<0.0001
	FC	0.0357	0.013	32.96	0.0066
	FH	0.0357	0.041	55.78	0.0007
	TMTC	-	-	-	-
gmRxrg	9-cis RA	0.0291	0.067	72.22	<0.0001
	TBT	0.0051	0.015	70.07	0.0001
	TPT	0.0357	0.029	47.24	<0.0001
	FC	0.0357	0.015	28.55	0.0021
	FH	0.0357	0.016	33.06	0.0088
	TMTC	-	-	-	-

* EC_{50} was not calculated as no plateau was reached

4.3.2 Differences in Rxr-LBD sequences between Atlantic cod and zebrafish

Due to the observed differences in ligand activation, the deduced amino acid sequences of the hinge-region and LBD of gmRxra, gmRxrb1, gmRxrb2, gmRxrb2d and gmRxrg were assessed through a multiple sequence alignment (Figure 17) (method 3.10). There are thirteen amino

acids that previously have been reported to be involved in binding of 9-cis RA in human RXR (Billas *et al.*, 2001; Tsuji, Shudo and Kagechika, 2015). Among these amino acids, only one difference in helix H3 is observed between the gmRxr-LBDs, i.e. gmRxrb1 has a substitution of alanine to threonine residue in position 68. Notably, gmRxrb1 and gmRxrb2 contain additional fourteen amino acids in helix 7, which is not present in gmRxra, gmRxrb2d, or gmRxrg. In helix 10, there is a cysteine residue that has been reported to be involved in anchoring organotins to the RXR-LBD through binding to the tin atom (Maire *et al.*, 2009). This amino acid is conserved in all subtypes.

An additional multiple sequence alignment was constructed for comparing the LBD of the gmRxr-subtypes to the two Rxrb orthologs (zfRxrbb and zfRxrba) in zebrafish, which previously have been demonstrated to not be activated by 9-cis-RA (Figure 18). These subtypes were also found to contain the same non-conserved Alanine residue as gmRxra, gmRxrb2 and gmRxrg. All the other residues involved in binding of 9-cis RA to Rxr were also conserved in zfRxrbb and zfRxrba, as well as the cysteine residue linked to organotin-anchoring in the ligand binding pocket. Importantly, the zfRxrb subtypes also contain an extended helix 7 as similar to gmRxrb1 and gmRxrb2.

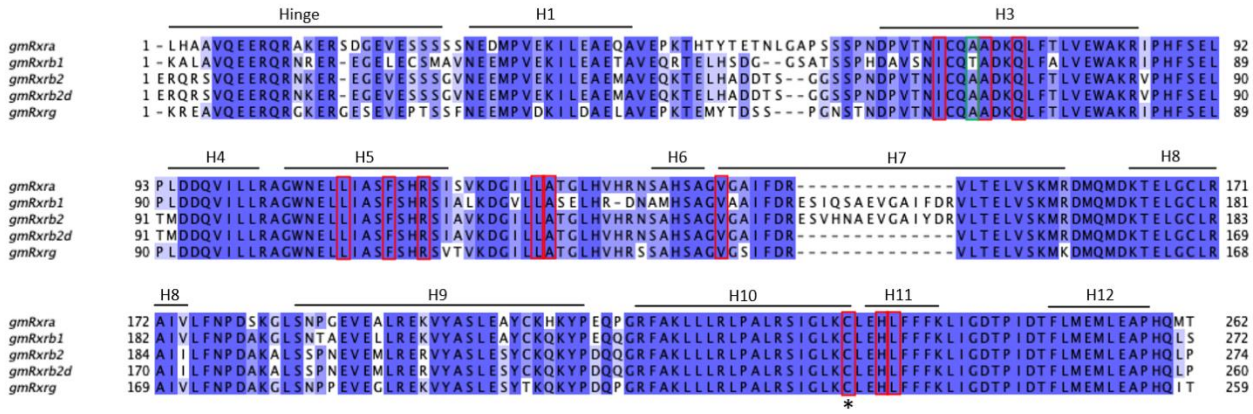

Figure 17: Multiple sequence alignment of gmRxra, gmRxrb1, gmRxrb2, gmRxrb2d and gmRxrg hinge-LBDs. Hinge-region and helices 1, 3-12 are indicated with black lines (H1, H3, H4, etc.). The blue coloring represents percentage identity between the sequences. Amino acids marked with red squares indicate conserved amino acids involved in 9-cis RA binding. Non-conserved amino acids involved in 9-cis RA binding are marked with a green square. The asterisk (*) under Cysteine indicates a residue involved in OTC-anchoring during Rxr binding. The multiple sequence alignment is produced in Clustal Omega and presented with JalView.

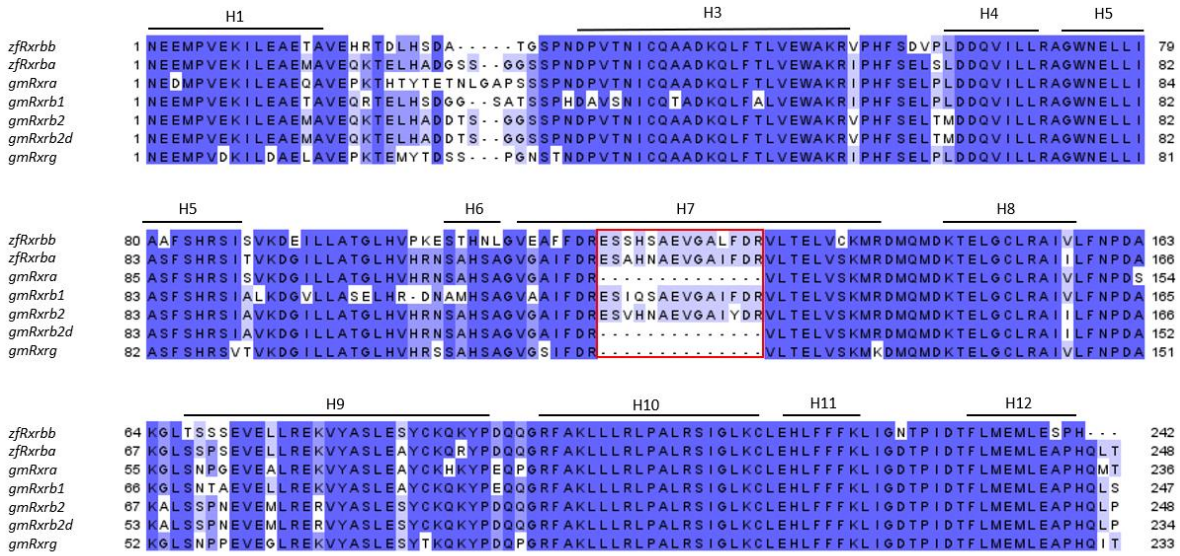

Figure 18: Multiple sequence alignment of LBD sequences from *D. rerio* Rxrbb and Rxrba (zfRxrbb and zfRxrba) and gmRxra/b1/b2/b2d/g. The fourteen-residue insert in H7 present in gmRxrb1/b2 is marked in a red square. The sequences of zfRxrbb, zfRxrba, gmRxrb1 and gmRxrb2 contain the insert. The blue coloring indicates percentage of amino acid identity. The alignment is produced in Clustal Omega and visualized in JalView.

4.4 Cytotoxicity and cell viability

A cytotoxicity assay was conducted for monitoring potential cytotoxic effects of the ligands on the COS-7 cells (method 3.13). The concentrations used for the cytotoxicity assay were identical to the concentrations used in the reporter gene assays. Triton X-100 (1 µM, 0.5 µM and 0.25 µM) was used as a positive control for cytotoxicity. As with the luciferase reporter gene assay, the exposure lasted for 24 hours. Membrane permeability and metabolic activity were measured with CFDA-AM and resazurin assay, respectively, (Figure 19). The results showed some variations, with only a few significant decreases in membrane permeability and metabolic activity at higher concentrations of TBT, fentin chloride, and fentin hydroxide.

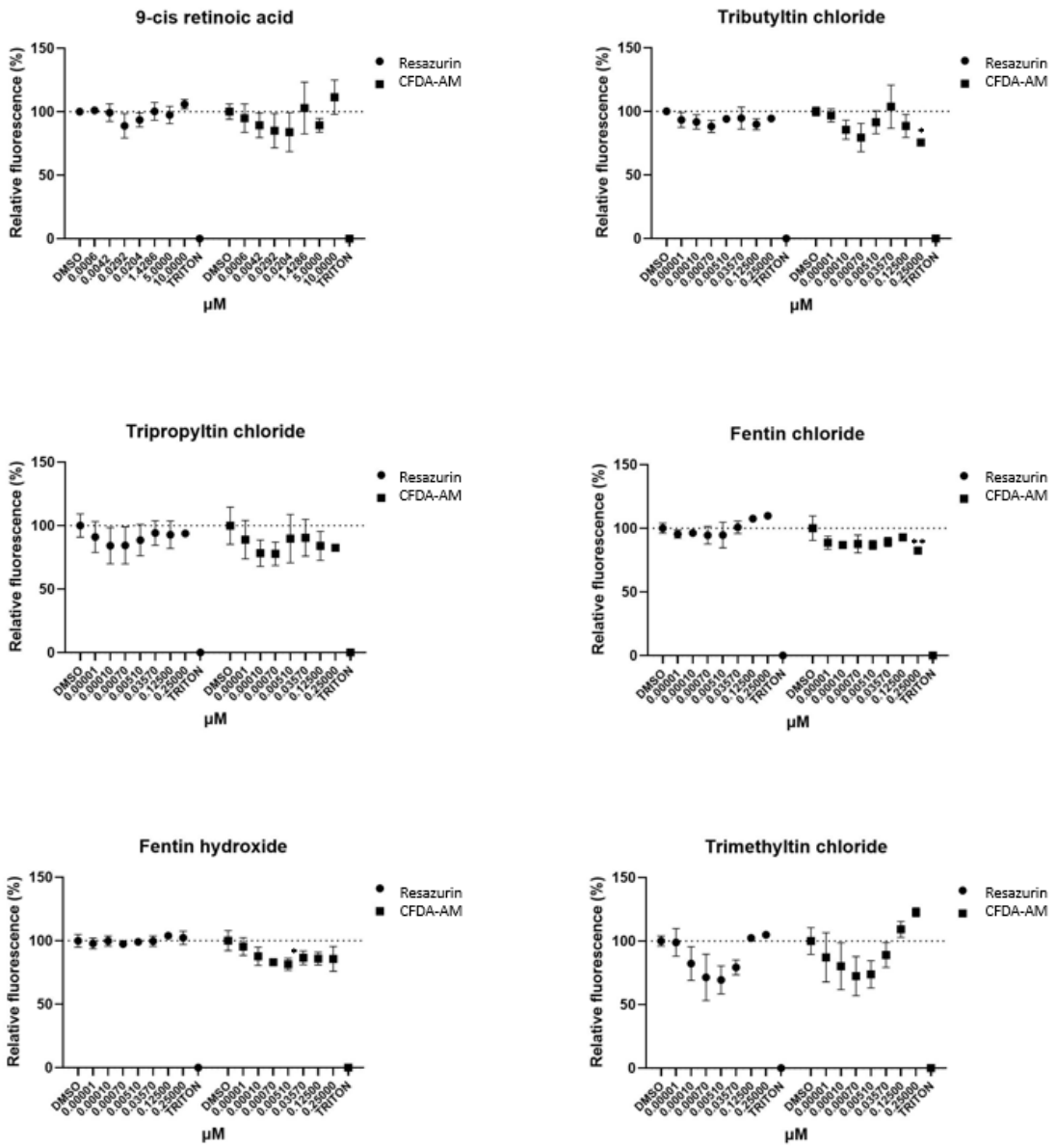

Figure 19: COS-7 cell viability after ligand exposure. Non-transfected COS-7 cells were exposed with 9-cis RA and TBT, TPT, FH, FC and TMTC at the same concentrations used in luciferase gene reporter assay, and as indicated in the figures. The dotted line represents the solvent control (DMEM with 0.5% DMSO), which was adjusted to 100%. Triton X-100 was used as a positive control of cytotoxicity. The round dots represent changes in metabolic activity (Resazurin), and the square dots represent changes in membrane permeability (CFDA-AM). Standard error of mean (SEM) is indicated. The statistical significance was calculated using Kruskal-Wallis test with Dunn's multiple comparisons test in GraphPad Prism 9, and statistical significance is indicated with asterisks "*": *=p≤0.05, **=p ≤0.01.

5. Discussion

This thesis has focused on studying Rxr nuclear receptors in Atlantic cod (gmRxr) with regard to their ligand activation capabilities to a known endogenous RXR ligand, i.e. 9-cis RA, and several organotins as potential exogenous ligands. Organotins are environmental pollutants with potent endocrine disrupting properties. In addition, they possess physico-chemical properties that make them resistant to degradation in the environment, and especially in marine environments due to their widespread historical use in antifouling paints on ships and the extended half-life of these compounds in sediments and seawater. Since organotins can enter marine food webs, it is important to increase our understanding of how these compounds interact with cellular signaling molecules, such as Rxr, and modulate the Rxr-signaling pathway. Such knowledge may shed light on the potential adverse effects organotins can have on Atlantic cod, and potentially also other marine teleost species. In this study, I have shown that gmRxra, gmRxrb2d and gmRxrg were transactivated *in vitro* by 9-cis RA, as well as by all the organotins tested, with the exception of TMTC. In contrast, gmRxrb1 and gmRxrb2 showed no significant activation for any of the ligands used. Since gmRxrb1 and gmRxrg have previously been cloned from Atlantic cod, the two last known subtypes gmRxra and gmRxrb2 have been the main focus of my work. gmRxrb2d was a new and interesting splice variant discovered in this thesis.

5.1 Cloning of gmRxra and gmRxrb2, and identification of an Rxrb2 splice variant (gmRxrb2d)

The subtypes gmRxrb1 and gmRxrg have previously been cloned from Atlantic cod and appear to be the most abundant and ubiquitously expressed subtypes based on previous research on normalized mRNA expression (Borge, 2021). gmRxrb1 was the subtype expressed at the highest levels in most tissues. gmRxrg and gmRxrb2 were moderately expressed across several tissues, but demonstrated the highest levels of expression in muscle and brain, respectively. gmRxra was by far the least expressed subtype, but showed some expression in heart tissue. Based on this knowledge, RNA extraction for cloning of gmRxra and gmRxrb2 were in this thesis performed with heart and brain tissue, respectively.

When cloning the gmRxrb2 subtype, a gmRxrb2 variant lacking a part (14 aa) of exon 8 (based on the exon-intron mapping by Borge, 2021) was simultaneously cloned. This variant was sequenced from several independent clones and was thus considered as a gmRxrb2 splice

variant denoted as gmRxrb2d. This finding was unexpected and an interesting addition to this thesis. Information on alternative splice variants of RXR receptors from any species is scarce, but likely important due to the receptors' central role in many physiological processes, including as a heterodimerization partner for other nuclear receptors. To my knowledge, this splice variant has not been reported previously in Atlantic cod, nor in any other teleost species. However, three different splice variants (isoforms) of RXRb have been recognized in humans (hRXRb1, hRXRb2 and hRXRb3) (as reviewed by Mukha, Kalkhoven and van Mil, 2021). The hRXRb2 isoform contains a longer N-terminal when compared to the canonical (full-length) hRXRb1 isoform. hRXRb3 contains an in-frame insertion of four amino acids (SRSL) in the LBD (Rana, Pearson and Redfern, 2001). It is unknown if the human splice variants affect binding and activation to ligands such as 9-cis RA, however it has been suggested that the SRSL insert may inhibit ligand binding.

5.2.1 Activation of gmRxra/b1/b2/b2d/g by 9-cis retinoic acid

Luciferase reporter gene assays were established in this thesis to obtain ligand-activation profiles for gmRxra, gmRxrb1, gmRxrb2, gmRxrb2d and gmRxrg, and to perform a comparative study regarding 9-cis RA and five different organotin compounds. The luciferase reporter gene assay is a GAL4-UAS based system where the LBD from Rxr is fused to the DNA-binding domain of GAL4, a transcription factor originating from yeast that binds to the specific regulatory sequence UAS (upstream activation sequence) found in the promoter region of its target genes. This system was chosen as the preferred method of assessing ligand-activation profiles due to several factors. By using UAS as an exogenous response element from yeast, the potential interference of endogenous compounds in the COS-7 cell line will be minimized. Also, the UAS usually leads to higher levels of downstream gene expression than endogenous tissue-specific promoters, which results in increased sensitivity of the assay (Yamada *et al.*, 2020).

To assess ligand activation of the receptors, COS-7 cells were transfected with the pCMX-GAL4-gmRxra/b1/b2/b2d/g eukaryotic expression plasmids and exposed to 9-cis RA, TBT, TPT, FC, FH and TMTC. 9-cis RA is a well-known and assumed endogenous ligand from other species, and this agonist has been widely used in previous studies. Borge (2021) also indicated 9-cis RA as a potential endogenous ligand in Atlantic cod, as the compound transactivated gmRxrg. However, the same study found no significant activation of gmRxrb1 when exposed

to 9-cis RA. Accordingly, 9-cis RA significantly transactivated gmRxrg at concentrations of 0.02 µM and higher, and there was no significant transactivation of neither gmRxrb1 nor gmRxrb2.The absence of transactivation of gmRxrb1 and gmRxrb2 could have been due to not being transcribed and synthesized in the transfected COS-7 cells. However, Western blot analyses verified that the fusion proteins in the transfected cells were synthesized, making it more likely that these receptors did not respond to the ligands tested. Interestingly, the gmRxrb2 splice variant, gmRxrb2d, was significantly transactivated when exposed to 9-cis RA, with a LOEC of 0.2 µM. The subtype gmRxra was also significantly transactivated by 9-cis RA with a LOEC of 0.02 µM. gmRxra demonstrated also the highest maximum fold activation with an E_{max} of 292, in comparison to gmRxrb2d and gmRxrg with an E_{max} of 176 and 72, respectively. EC_{50} values were not calculated for gmRxrb2d, as a plateau of activation was not reached, whilst the EC_{50} values for gmRxra and gmRxrg were 0.70 µM and 0.06 µM, respectively. Studies reporting 9-cis RA EC_{50} values in regard to other species are scarce. However, an EC_{50} value of 0.01 µM has been determined for hRXRa with a GAL4-hRXRa-LBD reporter gene assay in JEG3- cells (Nakanishi *et al.*, 2005), which is very similar to the EC_{50} value of gmRxra. In future studies it might be worth testing increased concentrations of 9-cis RA to potentially reach a plateau for calculation of EC_{50} values for gmRxrb2d.

5.2.2 Activation of gmRxra/b1/b2/b2d/g by organotins

Organotins have long been recognized as potent RXR agonists, with the most known compound being TBT. TBT has been linked to imposex induction in marine gastropods through disruption of the RXR signaling pathway. Regulations on the production and use of organotins, for instance global bans, have been implemented and have led to a significant decrease of TBT levels in marine waters. However, there are indications of illegal production and use of TBT, in addition to areas that still have high levels of organotins bound in sediments that can be released over time. The organotins TBT, TPT, FC, FH and TMTC were selected for this study, as these have been used previously in antifouling agents and are present in marine environments. The concentrations used in this study are similar to environmental levels that have been shown to cause adverse health effects in gastropods.

The subtypes gmRxra, gmRxrb2d and gmRxrg were activated by TBT, TPT, FC, and FH. TBT was the most potent compound for all activated receptors, causing significant activation at a lower concentration (LOEC: 0.0051 µM) than the other organotins. gmRxra demonstrated an

E_{max} of 510-fold activation after TBT exposure, which was the highest E_{max} among all receptors. gmRxrb2d and gmRxrg activation levels for TBT were lower, with an E_{max} of 177- and 70-fold activation, respectively. Moreover, the EC_{50} values for TBT and gmRxra, gmRxrg, and gmRxrb2d were quite similar at 0.016 µM, 0.015 µM, and 0.058 µM, respectively. gmRxra was the subtype demonstrating the lowest LOEC (0.0051 µM) for TBT, TPT, FC and FH. Based on the LOEC values and the high E_{max} values, gmRxra was the most sensitive and most responsive subtype to organotin exposure in the luciferase reporter gene assay. TPT was the second-most potent compound, causing significant activation of gmRxra and gmRxrb2d at 0.0051 µM, and for gmRxrg at 0.0357 µM. gmRxrb2d and gmRxrg were less sensitive to FC and FH than TBT and TPT, indicating that TBT and TPT are more potent agonists of gmRxra/b2d/g.

Interestingly, TBT, TPT, FC and FH have all in common that they produced high E_{max}-values (receptor activation) at quite low concentrations, also in comparison to the endogenous ligand 9-cis RA, where higher concentrations were needed to produce similar transactivation responses. This indicates a higher activation potential for organotins compared to 9-cis RA. In general, the low EC_{50}, low LOECs, and high E_{max} values produced by organotins at ng concentrations, indicate both high potency and efficacy for Atlantic cod Rxra, Rxrb2d and Rxrg. TMTC was the only organotin that did not transactivate any of the Rxr subtypes. However, TMTC has been important as a model toxicant in regard to central nervous system toxicity. Chen *et al.* performed a study in 2011 on TMTC neurobehavioral toxicity in embryonic zebrafish and found morphological and behavioral sensitivity for this compound. For instance, 5 µM TMTC exposure from 48 to 72 hours post-fertilization (hpf) resulted in significant promotion of apoptosis in the tail. This tail apoptosis has also been observed in embryos of the marine teleost *Sebastiscus marmoratus* when exposed to environmental organotin levels (0.1-10 ng/L) (Zhang *et al.*, 2011). However, this was induced by TBT, and this exposure induced Rxra expression in embryos exposed to 0.1 and 1 ng/L. This study might also indicate a link between TBT-induced tail abnormality and apoptosis. Even though TMTC did not transactivate gmRxr in my study, it is likely that this compound can cause adverse health effects related to another MoA than disruption of Rxr signaling. Based on previous research and the observed organotin-mediated transactivation of Atlantic cod Rxr at low concentrations (ng/L) used in this thesis, it is likely that these compounds have the potential to cause adverse effects through modulation of the Rxr-signaling pathway. There exist some studies regarding other teleosts and their exposure to organotins, including zebrafish. Organotins binding to Rxr in zebrafish has

been linked to Rxr signaling disruption, and therefore also disruption of CYP19 synthesis and altered estrogen metabolism. This was linked to aromatase inhibition, and ultimately, masculinization of female zebrafish (Cheshenko *et al.*, 2008).

5.2.3 Differences in amino acid sequences that affect ligand binding

The amino acid sequences of gmRxra, gmRxrb1, gmRxrb2, gmRxrb2d and gmRxrg were compared with a multiple sequence alignment to assess if differences in the primary structure could aid the explanation of the variation in ligand activation. Most amino acid residues shown in human RXRs to be involved in recognition and binding of 9-cis RA were conserved among the gmRxr subtypes. The only exception was the amino acid substitution of alanine to threonine in position 68 in helix 3 in gmRxrb1. More strikingly, there is a relatively well conserved region of fourteen additional amino acids in Helix 7 that is specific to gmRxrb1 and gmRxrb2, where 11 of the 14 residues are identical between the two receptors. gmRxrb1 and gmRxrb2 were the subtypes that were neither activated by 9-cis RA nor the organotins. Notably, the gmRxrb2 splice variant, gmRxrb2d, lacks this stretch of 14 amino acid residues in Helix 7, and in contrast to the canonical gmRxrb2 subtype, this variant was responsive to activation by both 9-cis RA and the organotins. This finding pinpoint that the removal of the 14 amino acid residues in Helix 7 is crucial for gmRxrb2 binding and activation by both endogenous and exogenous ligands. It is not unlikely that the same is evident also for the gmRxrb1 variant, but it still remains to identify a similar splice variant of this subtype.

Zebrafish have also numerous Rxr subtypes, including rxraa, rxrab, rxrba, rxrbb, rxrga and rxrgb (Oliveira *et al.*, 2013; Tao *et al.*, 2020). Notably, the subtypes zfRxrba and zfRxrbb have been reported to not bind 9-cis retinoic acid due to structural differences in the ligand binding domain (Jones *et al.*, 1995). Therefore, the amino acid sequences of the two Rxrb subtypes from zebrafish, i.e. zfRxrbb and zfRxrba, were obtained from the UniProt database and aligned with gmRxra, gmRxrb1, gmRxrb2, gmRxrb2d and gmRxrg. Interestingly, both of the zebrafish Rxrb subtypes contain the fourteen amino acid stretch within Helix 7 in the LBD as similar to gmRxrb1 and gmRxrb2. Based on our observations with the active gmRxrb2d splice variant, this stretch of amino acids appear to be the determinant factor of transcriptional activation, and its removal might also be necessary for the binding and activation of zfRxrba and zfRxrbb by 9-cis RA and organotins.

5.3 Conclusion

In this study, two Atlantic cod Rxr subtypes, gmRxra and gmRxrb2 were cloned from heart and brain tissue, respectively, and a luciferase-based *in vitro* reporter gene assay was established to assess ligand-activation by 9-cis RA and organotins. This was followed up by transactivation analyses of all gmRxr subtypes, including gmRxra, gmRxrb1, gmRxrb2 and gmRxrg, as well as a gmRxrb2 splice variant that was detected during gene cloning (gmRxrb2d). gmRxra, gmRxrb2d and gmRxrg showed significant activation by 9-cis RA and all the organotins tested, except TMTC. TBT was the most potent organotin agonist across receptors, and gmRxra was the most sensitive subtype. On the contrary, gmRxrb1 and gmRxrb2 showed no significant activation to any of the ligands after exposure. The lack of activation was identified to be due to a 14 amino acid stretch present in Helix 7, which was not present in the ligand-responsive gmRxrb2d splice variant. The unresponsiveness of gmRxrb1 and gmRxrb2 to ligand activation may indicate that these subtypes act solely as heterodimeric partners, and therefore might only be transactivated when interacting with a ligand-bound partner protein, such as RAR, PXR and PPAR.

The high potency of organotins in inducing gmRxra, gmRxrb2d and gmRxrg transactivation shows the ability of these compounds to potentially cause adverse health effects through modulation the Rxr signaling pathway in Atlantic cod, even at low concentrations. Organotins should therefore be considered a potential risk to marine teleosts and ecosystems. Even though the concentration levels organotins in general are decreasing, there still exists organotin hotspots along the Norwegian coast and globally. Therefore, continuous monitoring of the organotin concentrations in these hotspots is important.

5.4 Future perspectives

This study has provided new information regarding the Rxr subtypes in Atlantic cod and their activation potential when exposed to 9-cis RA and selected organotins. This is an area with limited knowledge. Continuous research regarding functional characterization of not only Atlantic cod receptors, but also NRs in general, is important for detecting potential adverse health effects on cellular signaling systems by environmental pollutants.

gmRxra, gmRxrb1, gmRxrb2, gmRxrb2d and gmRxrg were established with a UAS/GAL4-based reporter gene assay. This is a relatively high-throughput assay that could also be used for testing other potential Rxr ligands, such as LG100268 and bexarotene, or other potential exogenous compounds found in the environment, including PFAS. Furthermore, the UAS/GAL4-based reporter gene assay can be used for functional analyses in combination with in vitro mutagenesis. In vitro mutagenesis could be performed to remove the 14 amino acids in Helix 7 of gmRxrb1, and thereafter assess the potential ligand activation of this subtype when it resembles the Rxr subtypes that becomes ligand activated. Broader phylogenetic analyses with Rxr from a wide range of species could also be interesting for analyzing the similarity of Rxrb across evolution regarding the occurrence of an extended Helix 7 in comparison to the other Rxr subtypes. In silico structural analyses of Rxr proteins could also contribute to understand the importance of the amino acid stretch in Helix 7 in ligand binding, for instance via 9-cis RA docking simulations and molecular dynamics simulations. Further research into identifying other splice variants would also be interesting, as there might be more splice variants of gmRxr than the gmRxrb2 variant found in this study.

In situ hybridization could be performed for detecting gmRxr expression during embryonic and larval stages, which has been studied to some extent in zebrafish. As an alternative to *in vivo* studies, primary cell-cultures and tissue exposures could be used for studying adult Atlantic cod. For instance, precision-cut liver slices (PCLS) could be performed to study activation of the Rxr signaling pathway in combination with gene- and protein expression.

6. References

Aranda, A. and Pascual, A. (2001) 'Nuclear hormone receptors and gene expression', *Physiological Reviews*, 81(3), pp. 1269–1304. Available at: https://doi.org/10.1152/PHYSREV.2001.81.3.1269.

Beinsteiner, B., Markov, G. V., Bourguet, M., McEwen, A.G., Erb, S., Patel, A.K.M., El Khaloufi El Khaddar, F.Z., Lecroisey, C., Holzer, G., Essabri, K., Hazemann, I., Hamiche, A., Cianférani, S., Moras, D., Laudet, V. and Billas, I.M.L. (2022) 'A novel nuclear receptor subfamily enlightens the origin of heterodimerization', *BMC Biology*, 20(1), pp. 1–19. Available at: https://doi.org/10.1186/S12915-022-01413-0/FIGURES/7.

Bettin, C., Oehlmann, J. and Stroben, E. (1996) 'TBT-induced imposex in marine neogastropods is mediated by an increasing androgen level', *Helgolander Meeresuntersuchungen*, 50(3), pp. 299–317. Available at: https://doi.org/10.1007/bf02367105.

Beyer, J., Song, Y., Tollefsen, K.E., Berge, J.A., Tveiten, L., Helland, A., Øxnevad, S. and Schøyen, M. (2022) 'The ecotoxicology of marine tributyltin (TBT) hotspots: A review', *Marine Environmental Research*. Elsevier Ltd. Available at: https://doi.org/10.1016/j.marenvres.2022.105689.

Billas, I.M.L., Moulinier, L., Rochel, N. and Moras, D. (2001) 'Crystal Structure of the Ligand-binding Domain of the Ultraspiracle Protein USP, the Ortholog of Retinoid X Receptors in Insects', *Journal of Biological Chemistry*, 276(10), pp. 7465–7474. Available at: https://doi.org/10.1074/jbc.M008926200.

Blaber, S.J.M. (1970) 'THE OCCURRENCE OF A PENIS-LIKE OUTGROWTH BEHIND THE RIGHT TENTACLE IN SPENT FEMALES OF NUCELLA LAPILLUS (L.)', *Journal of Molluscan Studies*, 39(2–3), pp. 231–233. Available at: https://doi.org/10.1093/oxfordjournals.mollus.a065097.

Boehm, M.F., Zhang, L., Zhi, L., McClurg, M.R., Berger, E., Wagoner, M., Mais, D.E., Suto, C.M., Davies, P.J.A., Heyman, R.A. and Nadzan, A.M. (1995) 'Design and Synthesis of Potent Retinoid X Receptor Selective Ligands That Induce Apoptosis in Leukemia Cells', *Journal of Medicinal Chemistry*, 38(16), pp. 3146–3155. Available at: https://doi.org/10.1021/jm00016a018.

Borge, A. (2021) 'Identification and characterization of retinoid X receptors (RXR) in Atlantic cod (*Gadus morhua*) and their response to organic tin exposure'. Master's thesis. University of Bergen.

Brändli, R.C., Breedveld, G.D. and Cornelissen, G. (2009) 'Tributyltin sorption to marine sedimentary black carbon and to amended activated carbon', *Environmental Toxicology and Chemistry*, 28(3), pp. 503–508. Available at: https://doi.org/10.1897/08-236.1.

Castro, L.F.C., Lima, D., Machado, A., Melo, C., Hiromori, Y., Nishikawa, J., Nakanishi, T., Reis-Henriques, M.A. and Santos, M.M. (2007) 'Imposex induction is mediated through the Retinoid X Receptor signalling pathway in the neogastropod Nucella lapillus', *Aquatic Toxicology*, 85(1), pp. 57–66. Available at: https://doi.org/10.1016/J.AQUATOX.2007.07.016.

Cesario, R.M., Klausing, K., Razzaghi, H., Crombie, D., Rungta, D., Heyman, R.A. and Lala, D.S. (2001) 'The Rexinoid LG100754 Is a Novel RXR:PPARγ Agonist and Decreases Glucose Levels in Vivo', *Molecular Endocrinology*, 15(8), pp. 1360–1369. Available at: https://doi.org/10.1210/mend.15.8.0677.

Chen, J., Huang, C., Zheng, L., Simonich, M., Bai, C., Tanguay, R. and Dong, Q. (2011) 'Trimethyltin chloride (TMT) neurobehavioral toxicity in embryonic zebrafish', *Neurotoxicology and Teratology*, 33(6), pp. 721–726. Available at: https://doi.org/10.1016/j.ntt.2011.09.003.

Chen, L., Wu, L., Zhu, L. and Zhao, Y. (2018) 'Overview of the structure-based non-genomic effects of the nuclear receptor RXRα', *Cellular and Molecular Biology Letters*, 23(1), pp. 1–13. Available at: https://doi.org/10.1186/S11658-018-0103-3/TABLES/4.

Cheshenko, K., Pakdel, F., Segner, H., Kah, O. and Eggen, R.I.L. (2008) 'Interference of endocrine disrupting chemicals with aromatase CYP19 expression or activity, and consequences for reproduction

of teleost fish', *General and Comparative Endocrinology*, 155(1), pp. 31–62. Available at: https://doi.org/10.1016/J.YGCEN.2007.03.005.

Cunha, V., Santos, M.M., Moradas-Ferreira, P., Castro, L.F.C. and Ferreira, M. (2017) 'Simvastatin modulates gene expression of key receptors in zebrafish embryos', *Journal of Toxicology and Environmental Health - Part A: Current Issues*, 80(9), pp. 465–476. Available at: https://doi.org/10.1080/15287394.2017.1335258.

Dawson, M.I. and Xia, Z. (2012) 'The retinoid X receptors and their ligands', *Biochimica et Biophysica Acta - Molecular and Cell Biology of Lipids*, 1821(1), pp. 21–56. Available at: https://doi.org/10.1016/J.BBALIP.2011.09.014.

Diamanti-Kandarakis, E., Bourguignon, J.P., Giudice, L.C., Hauser, R., Prins, G.S., Soto, A.M., Zoeller, R.T. and Gore, A.C. (2009) 'Endocrine-disrupting chemicals: An Endocrine Society scientific statement', *Endocrine Reviews*. Oxford Academic, pp. 293–342. Available at: https://doi.org/10.1210/er.2009-0002.

Egea, P.F., Rochel, N., Birck, C., Vachette, P., Timmins, P.A. and Moras, D. (2001) 'Effects of ligand binding on the association properties and conformation in solution of retinoic acid receptors RXR and RAR', *Journal of Molecular Biology*, 307(2), pp. 557–576. Available at: https://doi.org/10.1006/JMBI.2000.4409.

Eide, M., Rydbeck, H., Tørresen, O.K., Lille-Langøy, R., Puntervoll, P., Goldstone, J. V, Jakobsen, K.S., Stegeman, J., Goksøyr, A. and Karlsen, O.A. (2018) 'Independent losses of a xenobiotic receptor across teleost evolution', *Scientific Reports*, 8(1). Available at: https://doi.org/10.1038/s41598-018-28498-4.

Ellingsen, K.E., Anderson, M.J., Shackell, N.L., Tveraa, T., Yoccoz, N.G. and Frank, K.T. (2015) 'The role of a dominant predator in shaping biodiversity over space and time in a marine ecosystem', *Journal of Animal Ecology*, 84(5), pp. 1242–1252. Available at: https://doi.org/10.1111/1365-2656.12396.

Fodor, I., Urbán, P., Scott, A.P. and Pirger, Z. (2020) 'A critical evaluation of some of the recent so-called "evidence" for the involvement of vertebrate-type sex steroids in the reproduction of mollusks', *Molecular and Cellular Endocrinology*, 516. Available at: https://doi.org/10.1016/J.MCE.2020.110949.

Hammill, M.O., Stenson, G.B., Swain, D.P. and Benoît, H.P. (2014) 'Feeding by grey seals on endangered stocks of Atlantic cod and white hake', in *ICES Journal of Marine Science*. Oxford Academic, pp. 1332–1341. Available at: https://doi.org/10.1093/icesjms/fsu123.

Hansen, C., Skern-Mauritzen, M., van der Meeren, G.I., Jahkel, A. and Drinkwater, K. (2016) 'Set-up of the Nordic and Barents Seas (NoBa) Atlantis model', *Fisken og havet*, nr.2/2016, p. 110. Available at: http://www.imr.no/filarkiv/2016/04/fh-2-2016_noba_atlantis_model_til_web.pdf/nb-no (Accessed: 15 March 2023).

Higuera-Ruiz, R. and Elorza, J. (2011) 'Shell thickening and chambering in the oyster Crassostrea gigas: Natural and anthropogenic influence of tributyltin contamination', *Environmental Technology*, 32(6), pp. 583–591. Available at: https://doi.org/10.1080/09593330.2010.506201.

Hoch, M. (2001) 'Organotin compounds in the environment - An overview', *Applied Geochemistry*. Pergamon, pp. 719–743. Available at: https://doi.org/10.1016/S0883-2927(00)00067-6.

Huang, J.H. and Matzner, E. (2004) 'Degradation of organotin compounds in organic and mineral forest soils', *Journal of Plant Nutrition and Soil Science*, 167(1), pp. 33–38. Available at: https://doi.org/10.1002/jpln.200321243.

Huang, W., Wu, Q., Xu, F., Li, L., Li, J., Que, H. and Zhang, G. (2020) 'Functional characterization of retinoid X receptor with an emphasis on the mediation of organotin poisoning in the Pacific oyster (Crassostrea gigas)', *Gene*, 753. Available at: https://doi.org/10.1016/J.GENE.2020.144780.

Hung, H., Katsoyiannis, A.A., Brorström-Lundén, E., Olafsdottir, K., Aas, W., Breivik, K., Bohlin-Nizzetto, P., Sigurdsson, A., Hakola, H., Bossi, R., Skov, H., Sverko, E., Barresi, E., Fellin, P. and Wilson, S. (2016) 'Temporal trends of Persistent Organic Pollutants (POPs) in arctic air: 20 years of monitoring under the Arctic Monitoring and Assessment Programme (AMAP)', *Environmental Pollution*, 217, pp. 52–61. Available at: https://doi.org/10.1016/j.envpol.2016.01.079.

Ijpenberg, A., Tan, N.S., Gelman, L., Kersten, S., Seydoux, J., Xu, J., Metzger, D., Canaple, L., Chambon, P., Wahli, W. and Desvergne, B. (2004) 'In vivo activation of PPAR target genes by RXR homodimers', *EMBO Journal*, 23(10), pp. 2083–2091. Available at: https://doi.org/10.1038/sj.emboj.7600209.

Ishigami-Yuasa, M. and Kagechika, H. (2020) 'Chemical screening of nuclear receptor modulators', *International Journal of Molecular Sciences*, 21(15), pp. 1–19. Available at: https://doi.org/10.3390/ijms21155512.

Jin, L. and Li, Y. (2010) 'Structural and functional insights into nuclear receptor signaling', *Advanced Drug Delivery Reviews*, pp. 1218–1226. Available at: https://doi.org/10.1016/j.addr.2010.08.007.

Johansen, S.D., Coucheron, D.H., Andreassen, M., Karlsen, B.O., Furmanek, T., Jørgensen, T.E., Emblem, Å., Breines, R., Nordeide, J.T., Moum, T., Nederbragt, A.J., Stenseth, N.C. and Jakobsen, K.S. (2009) 'Large-scale sequence analyses of Atlantic cod', *New Biotechnology*, pp. 263–271. Available at: https://doi.org/10.1016/j.nbt.2009.03.014.

Jones, B.B., Ohno, C.K., Allenby, G., Boffa, M.B., Levin, A.A., Grippo, J.F. and Petkovich, M. (1995) 'New retinoid X receptor subtypes in zebra fish (Danio rerio) differentially modulate transcription and do not bind 9-cis retinoic acid', *Molecular and Cellular Biology*, 15(10), pp. 5226–5234. Available at: https://doi.org/10.1128/mcb.15.10.5226.

Kahn, L.G., Harley, K.G., Siegel, E.L., Zhu, Y., Factor-Litva, P., Porucznik, C.A., Klein-Fedyshi, M. and Hipwell, A.E. (2021) 'Persistent organic pollutants and couple fecundability: a systematic review', *Human Reproduction Update*, pp. 339–366. Available at: https://doi.org/10.1093/humupd/dmaa037.

Karlsen, O.A., Puntervoll, P. and Goksøyr, A. (2012) 'Mass spectrometric analyses of microsomal cytochrome P450 isozymes isolated from β-naphthoflavone-treated Atlantic cod (Gadus morhua) liver reveal insights into the cod CYPome', *Aquatic Toxicology*, 108, pp. 2–10. Available at: https://doi.org/10.1016/j.aquatox.2011.08.018.

Kidd, K.A., Blanchfield, P.J., Mills, K.H., Palace, V.P., Evans, R.E., Lazorchak, J.M. and Flick, R.W. (2007) 'Collapse of a fish population after exposure to a synthetic estrogen', *Proceedings of the National Academy of Sciences of the United States of America*, 104(21), pp. 8897–8901. Available at: https://doi.org/10.1073/pnas.0609568104.

Kim, Y.A., Park, J.B., Woo, M.S., Lee, S.Y., Kim, H.Y. and Yoo, Y.H. (2019) 'Persistent organic pollutant-mediated insulin resistance', *International Journal of Environmental Research and Public Health*. MDPI AG. Available at: https://doi.org/10.3390/ijerph16030448.

Kojetin, D.J., Matta-Camacho, E., Hughes, T.S., Srinivasan, S., Nwachukwu, J.C., Cavett, V., Nowak, J., Chalmers, M.J., Marciano, D.P., Kamenecka, T.M., Shulman, A.I., Rance, M., Griffin, P.R., Bruning, J.B. and Nettles, K.W. (2015) 'Structural mechanism for signal transduction in RXR nuclear receptor heterodimers', *Nature Communications*, 6. Available at: https://doi.org/10.1038/ncomms9013.

Kristensen, M.L., Olsen, E.M., Moland, E., Knutsen, H., Grønkjær, P., Koed, A., Källo, K. and Aarestrup, K. (2021) 'Disparate movement behavior and feeding ecology in sympatric ecotypes of Atlantic cod', *Ecology and Evolution*, 11(16), pp. 11477–11490. Available at: https://doi.org/10.1002/ECE3.7939.

Langston, W.J., Pope, N.D., Davey, M., Langston, K.M., O' Hara, S.C.M., Gibbs, P.E. and Pascoe, P.L. (2015) 'Recovery from TBT pollution in English Channel environments: A problem solved?',

Marine Pollution Bulletin, 95(2), pp. 551–564. Available at: https://doi.org/10.1016/j.marpolbul.2014.12.011.

Laranjeiro, F., Sánchez-Marín, P., Oliveira, I.B., Galante-Oliveira, S. and Barroso, C. (2018) 'Fifteen years of imposex and tributyltin pollution monitoring along the Portuguese coast', *Environmental Pollution*, 232, pp. 411–421. Available at: https://doi.org/10.1016/j.envpol.2017.09.056.

Laudet, V. (2006) 'Nuclear Receptor Genes', in *eLS*. Wiley. Available at: https://doi.org/10.1038/npg.els.0006154.

Li, D., Yamada, T., Wang, F., Vulin, A.I. and Samuels, H.H. (2004) 'Novel Roles of Retinoid X Receptor (RXR) anal RXR Ligand in Dynamically Modulating the Activity of the Thyroid Hormone Receptor/RXR Heterodimer', *Journal of Biological Chemistry*, 279(9), pp. 7427–7437. Available at: https://doi.org/10.1074/JBC.M311596200.

Link, J.S., Bogstad, B., Sparholt, H. and Lilly, G.R. (2009) 'Trophic role of Atlantic cod in the ecosystem', *Fish and Fisheries*, pp. 58–87. Available at: https://doi.org/10.1111/j.1467-2979.2008.00295.x.

Liu, W., Zeng, M. and Fu, N. (2021) 'Functions of nuclear receptors SUMOylation', *Clinica Chimica Acta*. Elsevier B.V., pp. 27–33. Available at: https://doi.org/10.1016/j.cca.2021.01.007.

Madsen, A.K. (2016) 'Kloning, karakterisering og ligandaktivering av aryl hydrokarbonreseptor 2 (AHR2) fra Atlanterhavstorsk (*Gadus morhua*)'. Master's thesis. University of Bergen.

le Maire, A., Grimaldi, M., Roecklin, D., Dagnino, S., Vivat-Hannah, V., Balaguer, P. and Bourguet, W. (2009) 'Activation of RXR-PPAR heterodimers by organotin environmental endocrine disruptors', *EMBO Reports*, 10(4), pp. 367–373. Available at: https://doi.org/10.1038/embor.2009.8.

Maire, A. Le, Rey, M., Vivat, V., Guée, L., Blanc, P., Malosse, C., Chamot-Rooke, J., Germain, P. and Bourguet, W. (2022) 'Design and in vitro characterization of RXR variants as tools to investigate the biological role of endogenous rexinoids', *Journal of Molecular Endocrinology*, 69(3), pp. 377–390. Available at: https://doi.org/10.1530/JME-22-0021.

Matthiessen, P. and Gibbs, P.E. (1998) 'Critical appraisal of the evidence for tributyltin-mediated endocrine disruption in mollusks', *Environmental Toxicology and Chemistry*, 17(1), pp. 37–43. Available at: https://doi.org/10.1002/ETC.5620170106.

Moldoveanu, S. and David, V. (2021) *Modern Sample Preparation for Chromatography*. 2nd edn, *Modern Sample Preparation for Chromatography*. 2nd edn. Elsevier. Available at: https://doi.org/10.1016/B978-0-12-821405-3.01001-7.

Mukha, A., Kalkhoven, E. and van Mil, S.W.C. (2021) 'Splice variants of metabolic nuclear receptors: Relevance for metabolic disease and therapeutic targeting', *Biochimica et Biophysica Acta (BBA) - Molecular Basis of Disease*, 1867(10), p. 166183. Available at: https://doi.org/10.1016/J.BBADIS.2021.166183.

Nakanishi, T., Nishikawa, J.I., Hiromori, Y., Yokoyama, H., Koyanagi, M., Takasuga, S., Ishizaki, J.I., Watanabe, M., Isa, S.I., Utoguchi, N., Itoh, N., Kohno, Y., Nishihara, T. and Tanaka, K. (2005) 'Trialkyltin compounds bind retinoid X receptor to alter human placental endocrine functions', *Molecular endocrinology (Baltimore, Md.)*, 19(10), pp. 2502–2516. Available at: https://doi.org/10.1210/ME.2004-0397.

Nathan Dunn, D. H. (2019). ZFIN Zebrafish Nomenclature Conventions.Retrieved from https://wiki.zfin.org/display/general/ZFIN+Zebrafish+Nomenclature+Conventions

Oliveira, E., Casado, M., Raldúa, D., Soares, A., Barata, C. and Piña, B. (2013) 'Retinoic acid receptors' expression and function during zebrafish early development', *Journal of Steroid Biochemistry and Molecular Biology*, 138, pp. 143–151. Available at: https://doi.org/10.1016/j.jsbmb.2013.03.011.

Östman, Ö., Eklöf, J., Eriksson, B.K., Olsson, J., Moksnes, P.O. and Bergström, U. (2016) 'Top-down control as important as nutrient enrichment for eutrophication effects in North Atlantic coastal ecosystems', *Journal of Applied Ecology*. John Wiley and Sons Inc, pp. 1138–1147. Available at: https://doi.org/10.1111/1365-2664.12654.

Pawlak, M., Lefebvre, P. and Staels, B. (2012) 'General molecular biology and architecture of nuclear receptors', *Current Topics in Medicinal Chemistry*, 12(6), p. 504. Available at: https://doi.org/10.2174/156802612799436641.

Paz-Villarraga, C.A., Castro, Í.B. and Fillmann, G. (2022) 'Biocides in antifouling paint formulations currently registered for use', *Environmental Science and Pollution Research*, 29(20), pp. 30090–30101. Available at: https://doi.org/10.1007/s11356-021-17662-5.

Pérez, E., Bourguet, W., Gronemeyer, H. and De Lera, A.R. (2012) 'Modulation of RXR function through ligand design', *Biochimica et Biophysica Acta (BBA) - Molecular and Cell Biology of Lipids*, 1821(1), pp. 57–69. Available at: https://doi.org/10.1016/J.BBALIP.2011.04.003.

Pougnet, F., Schäfer, J., Dutruch, L., Garnier, C., Tessier, E., Dang, D.H., Lanceleur, L., Mullot, J.U., Lenoble, V. and Blanc, G. (2014) 'Sources and historical record of tin and butyl-tin species in a Mediterranean bay (Toulon Bay, France)', *Environmental Science and Pollution Research*, 21(10), pp. 6640–6651. Available at: https://doi.org/10.1007/s11356-014-2576-6.

Querfeld, C., Nagelli, L. V, Rosen, S.T., Kuzel, T.M. and Guitart, J. (2006) 'Bexarotene in the treatment of cutaneous T-cell lymphoma', *Expert Opinion on Pharmacotherapy*, pp. 907–915. Available at: https://doi.org/10.1517/14656566.7.7.907.

Rana, B., Pearson, A.D.J. and Redfern, C.P.F. (2001) 'RXRβ isoforms in neuroblastoma cells and evidence for a novel 3′-end transcript', *FEBS Letters*, 506(1), pp. 39–44. Available at: https://doi.org/10.1016/S0014-5793(01)02882-4.

Rastinejad, F., Huang, P., Chandra, V. and Khorasanizadeh, S. (2013) 'Understanding nuclear receptor form and function using structural biology', *Journal of molecular endocrinology*, 51(3). Available at: https://doi.org/10.1530/JME-13-0173.

Schøyen, M., Green, N.W., Hjermann, D., Tveiten, L., Beylich, B., Øxnevad, S. and Beyer, J. (2019) 'Levels and trends of tributyltin (TBT) and imposex in dogwhelk (Nucella lapillus) along the Norwegian coastline from 1991 to 2017', *Marine Environmental Research*. Elsevier, pp. 1–8. Available at: https://doi.org/10.1016/j.marenvres.2018.11.011.

Sguotti, C., Otto, S.A., Frelat, R., Langbehn, T.J., Ryberg, M.P., Lindegren, M., Durant, J.M., Stenseth, N.C. and Möllmann, C. (2018) 'Catastrophic dynamics limit Atlantic cod recovery', *Proceedings of the Royal Society B: Biological Sciences*, 286(1898). Available at: https://doi.org/10.1098/rspb.2018.2877.

Sharma, S., Shen, T., Chitranshi, N., Gupta, Veer, Basavarajappa, D., Sarkar, S., Mirzaei, M., You, Y., Krezel, W., Graham, S.L. and Gupta, Vivek (2022) 'Retinoid X Receptor: Cellular and Biochemical Roles of Nuclear Receptor with a Focus on Neuropathological Involvement', *Molecular Neurobiology*, 59(4), p. 2027. Available at: https://doi.org/10.1007/S12035-021-02709-Y.

Smith, B.S. (1971) 'Sexuality in the american mud snail, nassarius obsoletus say', *Journal of Molluscan Studies*, 39(5), pp. 377–378. Available at: https://doi.org/10.1093/oxfordjournals.mollus.a065117.

Søfteland, L., Holen, E. and Olsvik, P.A. (2010) 'Toxicological application of primary hepatocyte cell cultures of Atlantic cod (Gadus morhua) - Effects of BNF, PCDD and Cd', *Comparative Biochemistry and Physiology - C Toxicology and Pharmacology*, 151(4), pp. 401–411. Available at: https://doi.org/10.1016/j.cbpc.2010.01.003.

Star, B. *et al.* (2011) 'The genome sequence of Atlantic cod reveals a unique immune system', *Nature*, 477(7363), pp. 207–210. Available at: https://doi.org/10.1038/nature10342.

Sunday, A.O., Alafara, B.A. and Oladele, O.G. (2012) 'Toxicity and speciation analysis of organotin compounds', *Chemical Speciation and Bioavailability*, 24(4), pp. 216–226. Available at: https://doi.org/10.3184/095422912X13491962881734.

Tallafuss, A., Hale, L.A., Yan, Y.L., Dudley, L., Eisen, J.S. and Postlethwait, J.H. (2006) 'Characterization of retinoid-X receptor genes rxra, rxrba, rxrbb and rxrg during zebrafish development', *Gene Expression Patterns*, 6(5), pp. 556–565. Available at: https://doi.org/10.1016/j.modgep.2005.10.005.

Tanaka, T. and De Luca, L.M. (2009) 'Therapeutic potential of "rexinoids" in cancer prevention and treatment', *Cancer Research*, 69(12), pp. 4945–4947. Available at: https://doi.org/10.1158/0008-5472.CAN-08-4407/655067/P/THERAPEUTIC-POTENTIAL-OF-REXINOIDS-IN-CANCER.

Tao, J., Bai, C., Chen, Y., Zhou, H., Liu, Y., Shi, Q., Pan, W., Dong, H., Li, L., Xu, H., Tanguay, R., Huang, C. and Dong, Q. (2020) 'Environmental relevant concentrations of benzophenone-3 induced developmental neurotoxicity in zebrafish'. Available at: https://doi.org/10.1016/j.scitotenv.2020.137686.

Tate, B.F., Allenby, G., Janocha, R., Kazmer, S., Speck, J., Sturzenbecker, L.J., Abarzúa, P., Levin, A.A. and Grippo, J.F. (1994) 'Distinct binding determinants for 9-cis retinoic acid are located within AF-2 of retinoic acid receptor alpha', *Molecular and Cellular Biology*, 14(4), pp. 2323–2330. Available at: https://doi.org/10.1128/mcb.14.4.2323-2330.1994.

Tsuji, M., Shudo, K. and Kagechika, H. (2015) 'Docking simulations suggest that all-trans retinoic acid could bind to retinoid X receptors', *Journal of Computer-Aided Molecular Design*, 29(10), pp. 975–988. Available at: https://doi.org/10.1007/s10822-015-9869-9.

van Gestel, C. A. M., Van Belleghem, F. G.A.J., van den Brink,N. W., Droge, S. T. J., Hamers, T., Hermens, J. L. M., Kraak, M. H. S., Löhr, A. J., Parsons, J. R., Ragas, A. M. J., van Straalen, N. M. og Vijver, M. G. (2019) *Environmental Toxicology, an open online textbook - Wikiwijs* (September, 2019). Available from: https://maken.wikiwijs.nl/147644/Environmental_Toxicology__an_open_online_textbook#!page-5414981.

Warford, L., Mason, C., Lonsdale, J., Bersuder, P., Blake, S., Evans, N., Thomas, B. and James, D. (2022) 'A reassessment of TBT action levels for determining the fate of dredged sediments in the United Kingdom', *Marine Pollution Bulletin*, 176. Available at: https://doi.org/10.1016/j.marpolbul.2022.113439.

Watanabe, M. and Kakuta, H. (2018) 'Retinoid X Receptor Antagonists', *International Journal of Molecular Sciences 2018, Vol. 19, Page 2354*, 19(8), p. 2354. Available at: https://doi.org/10.3390/IJMS19082354.

Waxman, J.S. and Yelon, D. (2007) 'Comparison of the expression patterns of newly identified zebrafish retinoic acid and retinoid X receptors', *Developmental Dynamics*, 236(2), pp. 587–595. Available at: https://doi.org/10.1002/dvdy.21049.

Weikum, E.R., Liu, X. and Ortlund, E.A. (2018) 'The nuclear receptor superfamily: A structural perspective', *Protein Science*, 27(11), pp. 1876–1892. Available at: https://doi.org/10.1002/PRO.3496.

Widdows, J. and Page, D.S. (1993) 'Effects of tributyltin and dibutyltin on the physiological energetics of the mussel, Mytilus edulis', *Marine Environmental Research*, 35(3), pp. 233–249. Available at: https://doi.org/10.1016/0141-1136(93)90096-I.

Wroblewski, J., Neis, B. and Gosse, K. (2005) 'Inshore stocks of Atlantic cod are important for rebuilding the East Coast fishery', *Coastal Management*, pp. 411–432. Available at: https://doi.org/10.1080/08920750500217930.

Yamada, M., Nagasaki, S.C., Suzuki, Y., Hirano, Y. and Imayoshi, I. (2020) 'Optimization of Light-Inducible Gal4/UAS Gene Expression System in Mammalian Cells', *iScience*, 23(9). Available at:

https://doi.org/10.1016/j.isci.2020.101506.

Yang, C., Li, Q. and Li, Y. (2014) ‘Targeting Nuclear Receptors with Marine Natural Products’, *Marine Drugs 2014, Vol. 12, Pages 601-635*, 12(2), pp. 601–635. Available at: https://doi.org/10.3390/MD12020601.

Zhang, J., Zuo, Z., Wang, Y., Yu, A., Chen, Y. and Wang, C. (2011) ‘Tributyltin chloride results in dorsal curvature in embryo development of Sebastiscus marmoratus via apoptosis pathway’, *Chemosphere*, 82(3), pp. 437–442. Available at: https://doi.org/10.1016/j.chemosphere.2010.09.057.

Zhang, S., Li, P. and Li, Z.-H. (2021) ‘Toxicity of organotin compounds and the ecological risk of organic tin with co-existing contaminants in aquatic organisms’, *Comparative Biochemistry and Physiology, Part C*, 246, p. 109054. Available at: https://doi.org/10.1016/j.cbpc.2021.109054.

Zou, C., Wang, L., Shu, C., Tan, X., Wu, Z., Zou, Y., Li, Z., Wang, G., Song, Z. and You, F. (2023) ‘Rxrs and their partner receptor genes inducing masculinization plausibly mediated by endocrine disruption in Paralichthys olivaceus’, *The Journal of Steroid Biochemistry and Molecular Biology*, 226, p. 106219. Available at: https://doi.org/10.1016/J.JSBMB.2022.106219.

Appendix

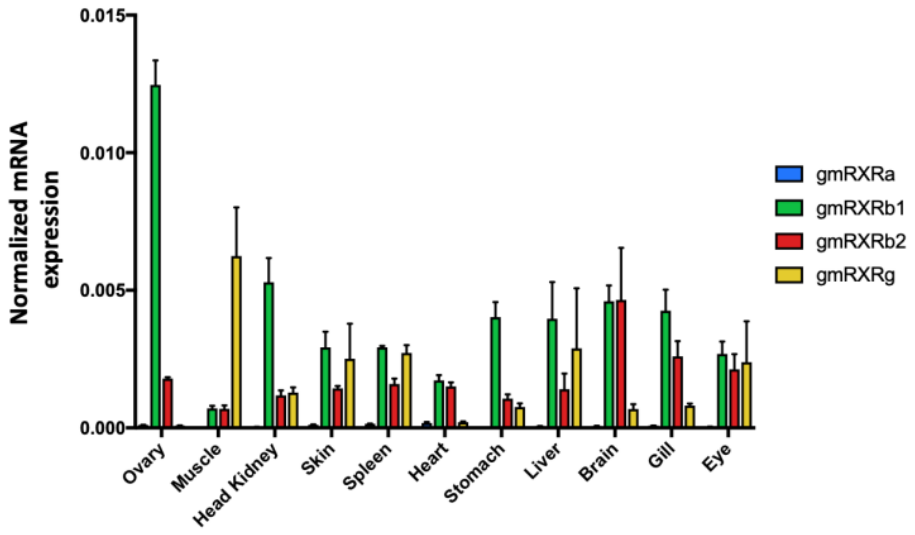

Figure A: Normalized mRNA expression of *gmrxr* isoforms in different tissues of Atlantic cod. Figure adapted from Borge, 2021.

Table A: P-values for the activated receptors gmRxra, gmRxrb2d and gmRxrg for all concentrations (10 µM, 5 µM, 1.42 µM, 0.20 µM, 0.02 µM, 0.0041 µM and 0.0005 µM) of 9-cis RA. The statistical significance was calculated using Kruskal-Wallis test with Dunn's multiple comparisons test in GraphPad Prism 9 and indicated with p-value. NS indicates no significance.

Receptor / 9-cis RA	10 µM	5 µM	1.42 µM	0.20 µM	0.02 µM	0.0041 µM	0.0005 µM
gmRxra	<0.0001	<0.0001	<0.0001	0.0002	0.0031	NS	NS
gmRxrb2d	<0.0001	<0.0001	<0.0001	0.0014	NS	NS	NS
gmRxrg	<0.0001	<0.0001	<0.0001	<0.0001	0.0220	NS	NS

Table B: P-values for the activated receptors gmRxra, gmRxrb2d and gmRxrg for all concentrations (0.25 µL, 0.125 µM, 0.0357 µM, 0.0051 µM, 0.0007 µM, 0.0001 µM and 0.00001 µM) of organotins. The statistical significance was calculated using Kruskal-Wallis test with Dunn's multiple comparisons test in GraphPad Prism 9. NS indicates no significance.

Receptor	OTC (µM)	0.25	0.125	0.0357	0.0051	0.0007	0.0001	0.00001
gmRxra	TBT	<0.0001	<0.0001	<0.0001	0.0005	NS	NS	NS
	TPT	<0.0001	<0.0001	<0.0001	0.0044	NS	NS	NS
	FC	<0.0001	<0.0001	<0.0001	0.0155	NS	NS	NS
	FH	<0.0001	<0.0001	<0.0001	0.0044	NS	NS	NS
	TMTC	NS	NS	NS	NS	NS	NS	NS
gmRxrb2d	TBT	<0.0001	<0.0001	<0.0001	0.0070	NS	NS	NS
	TPT	<0.0001	<0.0001	0.0009	0.0396	NS	NS	NS
	FC	0.0066	0.0021	0.0043	NS	NS	NS	NS
	FH	0.0007	<0.0001	0.0296	NS	NS	NS	NS
	TMTC	NS	NS	NS	NS	NS	NS	NS
gmRxrg	TBT	0.0001	<0.0001	0.0003	0.0076	NS	NS	NS
	TPT	<0.0001	<0.0001	0.0014	NS	NS	NS	NS
	FC	0.0021	<0.0001	0.0021	NS	NS	NS	NS
	FH	0.0088	0.0004	0.0064	NS	NS	NS	NS
	TMTC	NS	NS	NS	NS	NS	NS	NS